24 *Markov chain Monte Carlo (MCMC) inference*

24.1 Introduction

In Chapter 23, we introduced some simple Monte Carlo methods, including rejection sampling and importance sampling. The trouble with these methods is that they do not work well in high dimensional spaces. The most popular method for sampling from high-dimensional distributions is **Markov chain Monte Carlo** or **MCMC**. In a survey by *SIAM News*[1], MCMC was placed in the top 10 most important algorithms of the 20th century.

The basic idea behind MCMC is to construct a Markov chain (Section 17.2) on the state space $\mathcal{X}$ whose stationary distribution is the target density $p^*(\mathbf{x})$ of interest (this may be a prior or a posterior). That is, we perform a random walk on the state space, in such a way that the fraction of time we spend in each state $\mathbf{x}$ is proportional to $p^*(\mathbf{x})$. By drawing (correlated!) samples $\mathbf{x}_0, \mathbf{x}_1, \mathbf{x}_2, \ldots,$ from the chain, we can perform Monte Carlo integration wrt p^*. We give the details below.

The MCMC algorithm has an interesting history. It was discovered by physicists working on the atomic bomb at Los Alamos during World War II, and was first published in the open literature in (Metropolis et al. 1953) in a chemistry journal. An extension was published in the statistics literature in (Hastings 1970), but was largely unnoticed. A special case (Gibbs sampling, Section 24.2) was independently invented in 1984 in the context of Ising models and was published in (Geman and Geman 1984). But it was not until (Gelfand and Smith 1990) that the algorithm became well-known to the wider statistical community. Since then it has become wildly popular in Bayesian statistics, and is becoming increasingly popular in machine learning.

It is worth briefly comparing MCMC to variational inference (Chapter 21). The advantages of variational inference are (1) for small to medium problems, it is usually faster; (2) it is deterministic; (3) is it easy to determine when to stop; (4) it often provides a lower bound on the log likelihood. The advantages of sampling are: (1) it is often easier to implement; (2) it is applicable to a broader range of models, such as models whose size or structure changes depending on the values of certain variables (e.g., as happens in matching problems), or models without nice conjugate priors; (3) sampling can be faster than variational methods when applied to really huge models or datasets.[2]

1. Source: `http://www.siam.org/pdf/news/637.pdf`.

2. The reason is that sampling passes specific values of variables (or sets of variables), whereas in variational inference, we pass around distributions. Thus sampling passes sparse messages, whereas variational inference passes dense messages For comparisons of the two approaches, see e.g., (Yoshida and West 2010) and articles in (Bekkerman et al.

24.2 Gibbs sampling

In this section, we present one of the most popular MCMC algorithms, known as **Gibbs sampling**.[3] (In physics, this method is known as **Glauber dynamics** or the **heat bath** method.) This is the MCMC analog of coordinate descent.

24.2.1 Basic idea

The idea behind Gibbs sampling is that we sample each variable in turn, conditioned on the values of all the other variables in the distribution. That is, given a joint sample $\mathbf{x}^s$ of all the variables, we generate a new sample $\mathbf{x}^{s+1}$ by sampling each component in turn, based on the most recent values of the other variables. For example, if we have $D = 3$ variables, we use

- $x_1^{s+1} \sim p(x_1|x_2^s, x_3^s)$
- $x_2^{s+1} \sim p(x_2|x_1^{s+1}, x_3^s)$
- $x_3^{s+1} \sim p(x_3|x_1^{s+1}, x_2^{s+1})$

This readily generalizes to D variables. If x_i is a visible variable, we do not sample it, since its value is already known.

The expression $p(x_i|\mathbf{x}_{-i})$ is called the **full conditional** for variable i. In general, x_i may only depend on some of the other variables. If we represent $p(\mathbf{x})$ as a graphical model, we can infer the dependencies by looking at i's Markov blanket, which are its neighbors in the graph. Thus to sample x_i, we only need to know the values of i's neighbors. In this sense, Gibbs sampling is a distributed algorithm. However, it is not a parallel algorithm, since the samples must be generated sequentially.

For reasons that we will explain in Section 24.4.1, it is necessary to discard some of the initial samples until the Markov chain has **burned in**, or entered its stationary distribution. We discuss how to estimate when burnin has occured in Section 24.4.1. In the examples below, we just discard the initial 25% of the samples, for simplicity.

24.2.2 Example: Gibbs sampling for the Ising model

In Section 21.3.2, we applied mean field to an Ising model. Here we apply Gibbs sampling.

Gibbs sampling in pairwise MRF/CRF takes the form

$$p(x_t|\mathbf{x}_{-t}, \boldsymbol{\theta}) \propto \prod_{s \in \text{nbr}(t)} \psi_{st}(x_s, x_t) \tag{24.1}$$

In the case of an Ising model with edge potentials $\psi(x_s, x_t) = \exp(Jx_sx_t)$, where $x_t \in$

2011)

3. Josiah Willard Gibbs, 1839–1903, was an American physicist.

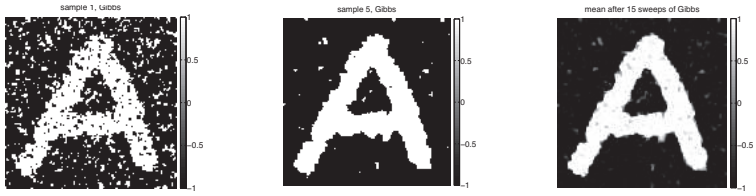

(a) (b) (c)

Figure 24.1 Example of image denoising. We use an Ising prior with $W_{ij} = J = 1$ and a Gaussian noise model with $\sigma = 2$. We use Gibbs sampling (Section 24.2) to perform approximate inference. (a) Sample from the posterior after one sweep over the image. (b) Sample after 5 sweeps. (c) Posterior mean, computed by averaging over 15 sweeps. Compare to Figure 21.3 which shows the results of using mean field inference. Figure generated by `isingImageDenoiseDemo`.

$\{-1, +1\}$, the full conditional becomes

$$p(x_t = +1|\mathbf{x}_{-t}, \boldsymbol{\theta}) = \frac{\prod_{s\in\text{nbr}(t)} \psi_{st}(x_t = +1, x_s)}{\prod_{s\in\text{nbr}(t)} \psi(s_t = +1, x_s) + \prod_{s\in\text{nbr}(t)} \psi(x_t = -1, x_s)} \tag{24.2}$$

$$= \frac{\exp[J \sum_{s\in\text{nbr}(t)} x_s]}{\exp[J \sum_{s\in\text{nbr}(t)} x_s] + \exp[-J \sum_{s\in\text{nbr}(t)} x_s]} \tag{24.3}$$

$$= \frac{\exp[J\eta_t]}{\exp[J\eta_t] + \exp[-J\eta_t]} = \text{sigm}(2J\eta_t) \tag{24.4}$$

where J is the coupling strength, $\eta_t \triangleq \sum_{s\in\text{nbr}(t)} x_t$ and $\text{sigm}(u) = 1/(1+e^{-u})$ is the sigmoid function. It is easy to see that $\eta_t = x_t(a_t - d_t)$, where a_t is the number of neighbors that agree with (have the same sign as) t, and d_t is the number of neighbors who disagree. If this number is equal, the "forces" on x_t cancel out, so the full conditional is uniform.

We can combine an Ising prior with a local evidence term ψ_t. For example, with a Gaussian observation model, we have $\psi_t(x_t) = \mathcal{N}(y_t|x_t, \sigma^2)$. The full conditional becomes

$$p(x_t = +1|\mathbf{x}_{-t}, \mathbf{y}, \boldsymbol{\theta}) = \frac{\exp[J\eta_t]\psi_t(+1)}{\exp[J\eta_t]\psi_t(+1) + \exp[-J\eta_t]\psi_t(-1)} \tag{24.5}$$

$$= \text{sigm}\left(2J\eta_t - \log\frac{\psi_t(+1)}{\psi_t(-1)}\right) \tag{24.6}$$

Now the probability of x_t entering each state is determined both by compatibility with its neighbors (the Ising prior) and compatibility with the data (the local likelihood term).

See Figure 24.1 for an example of this algorithm applied to a simple image denoising problem. The results are similar to mean field (Figure 21.3) except that the final estimate (based on averaging the samples) is somewhat "blurrier", due to the fact that mean field tends to be over-confident.

24.2.3 Example: Gibbs sampling for inferring the parameters of a GMM

It is straightforward to derive a Gibbs sampling algorithm to "fit" a mixture model, especially if we use conjugate priors. We will focus on the case of mixture of Gaussians, although the results are easily extended to other kinds of mixture models. (The derivation, which follows from the results of Section 4.6, is much easier than the corresponding variational Bayes algorithm in Section 21.6.1.)

Suppose we use a semi-conjugate prior. Then the full joint distribution is given by

$$p(\mathbf{x}, \mathbf{z}, \boldsymbol{\mu}, \boldsymbol{\Sigma}, \boldsymbol{\pi}) = p(\mathbf{x}|\mathbf{z}, \boldsymbol{\mu}, \boldsymbol{\Sigma}) p(\mathbf{z}|\boldsymbol{\pi}) p(\boldsymbol{\pi}) \prod_{k=1}^{K} p(\boldsymbol{\mu}_k) p(\boldsymbol{\Sigma}_k) \tag{24.7}$$

$$= \left(\prod_{i=1}^{N} \prod_{k=1}^{K} (\pi_k \mathcal{N}(\mathbf{x}_i|\boldsymbol{\mu}_k, \boldsymbol{\Sigma}_k))^{\mathbb{I}(z_i=k)} \right) \times \tag{24.8}$$

$$\mathrm{Dir}(\boldsymbol{\pi}|\boldsymbol{\alpha}) \prod_{k=1}^{K} \mathcal{N}(\boldsymbol{\mu}_k|\mathbf{m}_0, \mathbf{V}_0) \mathrm{IW}(\boldsymbol{\Sigma}_k|\mathbf{S}_0, \nu_0) \tag{24.9}$$

We use the same prior for each mixture component. The full conditionals are as follows. For the discrete indicators, we have

$$p(z_i = k|\mathbf{x}_i, \boldsymbol{\mu}, \boldsymbol{\Sigma}, \boldsymbol{\pi}) \propto \pi_k \mathcal{N}(\mathbf{x}_i|\boldsymbol{\mu}_k, \boldsymbol{\Sigma}_k) \tag{24.10}$$

For the mixing weights, we have (using results from Section 3.4)

$$p(\boldsymbol{\pi}|\mathbf{z}) = \mathrm{Dir}(\{\alpha_k + \sum_{i=1}^{N} \mathbb{I}(z_i = k)\}_{k=1}^{K}) \tag{24.11}$$

For the means, we have (using results from Section 4.6.1)

$$p(\boldsymbol{\mu}_k|\boldsymbol{\Sigma}_k, \mathbf{z}, \mathbf{x}) = \mathcal{N}(\boldsymbol{\mu}_k|\mathbf{m}_k, \mathbf{V}_k) \tag{24.12}$$

$$\mathbf{V}_k^{-1} = \mathbf{V}_0^{-1} + N_k \boldsymbol{\Sigma}_k^{-1} \tag{24.13}$$

$$\mathbf{m}_k = \mathbf{V}_k(\boldsymbol{\Sigma}_k^{-1} N_k \overline{\mathbf{x}}_k + \mathbf{V}_0^{-1} \mathbf{m}_0) \tag{24.14}$$

$$N_k \triangleq \sum_{i=1}^{N} \mathbb{I}(z_i = k) \tag{24.15}$$

$$\overline{\mathbf{x}}_k \triangleq \frac{\sum_{i=1}^{N} \mathbb{I}(z_i = k)\mathbf{x}_i}{N_k} \tag{24.16}$$

For the covariances, we have (using results from Section 4.6.2)

$$p(\boldsymbol{\Sigma}_k|\boldsymbol{\mu}_k, \mathbf{z}, \mathbf{x}) = \mathrm{IW}(\boldsymbol{\Sigma}_k|\mathbf{S}_k, \nu_k) \tag{24.17}$$

$$\mathbf{S}_k = \mathbf{S}_0 + \sum_{i=1}^{N} \mathbb{I}(z_i = k)(\mathbf{x}_i - \boldsymbol{\mu}_k)(\mathbf{x}_i - \boldsymbol{\mu}_k)^T \tag{24.18}$$

$$\nu_k = \nu_0 + N_k \tag{24.19}$$

See `gaussMissingFitGibbs` for some Matlab code. (This code can also sample missing values for $\mathbf{x}$, if necessary.)

24.2.3.1 Label switching

Although it is simple to implement, Gibbs sampling for mixture models has a fundamental weakness. The problem is that the parameters of the model $\boldsymbol{\theta}$, and the indicator functions $\mathbf{z}$, are unidentifiable, since we can arbitrarily permute the hidden labels without affecting the likelihood (see Section 11.3.1). Consequently, we cannot just take a Monte Carlo average of the samples to compute posterior means, since what one sample considers the parameters for cluster 1 may be what another sample considers the parameters for cluster 2. Indeed, if we could average over all modes, we would find $\mathbb{E}\left[\boldsymbol{\mu}_k|\mathcal{D}\right]$ is the same for all k (assuming a symmetric prior). This is called the **label switching** problem.

This problem does not arise in EM or VBEM, which just "lock on" to a single mode. However, it arises in any method that visits multiple modes. In 1d problems, one can try to prevent this problem by introducing constraints on the parameters to ensure identifiability, e.g., $\mu_1 < \mu_2 < \mu_3$ (Richardson and Green 1997). However, this does not always work, since the likelihood might overwhelm the prior and cause label switching anyway. Furthermore, this technique does not scale to higher dimensions. Another approach is to post-process the samples by searching for a global label permutation to apply to each sample that minimizes some loss function (Stephens 2000); however, this can be slow.

Perhaps the best solution is simply to "not ask" questions that cannot be uniquely identified. For example, instead of asking for the probability that data point i belongs to cluster k, ask for the probability that data points i and j belong to the same cluster. The latter question is invariant to the labeling. Furthermore, it only refers to observable quantities (are i and j grouped together or not), rather than referring to unobservable quantities, such as latent clusters. This approach has the further advantage that it extends to infinite mixture models, discussed in Section 25.2, where K is unbounded; in such models, the notion of a hidden cluster is not well defined, but the notion of a partitioning of the data *is* well defined

24.2.4 Collapsed Gibbs sampling *

In some cases, we can analytically integrate out some of the unknown quantities, and just sample the rest. This is called a **collapsed Gibbs sampler**, and it tends to be much more efficient, since it is sampling in a lower dimensional space.

More precisely, suppose we sample $\mathbf{z}$ and integrate out $\boldsymbol{\theta}$. Thus the $\boldsymbol{\theta}$ parameters do not participate in the Markov chain; consequently we can draw conditionally independent samples $\boldsymbol{\theta}^s \sim p(\boldsymbol{\theta}|\mathbf{z}^s, \mathcal{D})$, which will have much lower variance than samples drawn from the joint state space (Liu et al. 1994). This process is called **Rao-Blackwellisation**, named after the following theorem:

Theorem 24.2.1 (Rao-Blackwell)**.** *Let $\mathbf{z}$ and $\boldsymbol{\theta}$ be dependent random variables, and $f(\mathbf{z}, \boldsymbol{\theta})$ be some scalar function. Then*

$$\mathrm{var}_{\mathbf{z},\boldsymbol{\theta}}\left[f(\mathbf{z},\boldsymbol{\theta})\right] \geq \mathrm{var}_{\mathbf{z}}\left[\mathbb{E}_{\boldsymbol{\theta}}\left[f(\mathbf{z},\boldsymbol{\theta})|\mathbf{z}\right]\right] \tag{24.20}$$

This theorem guarantees that the variance of the estimate created by analytically integrating out $\boldsymbol{\theta}$ will always be lower (or rather, will never be higher) than the variance of a direct MC estimate. In collapsed Gibbs, we sample $\mathbf{z}$ with $\boldsymbol{\theta}$ integrated out; the above Rao-Blackwell theorem still applies in this case (Liu et al. 1994).

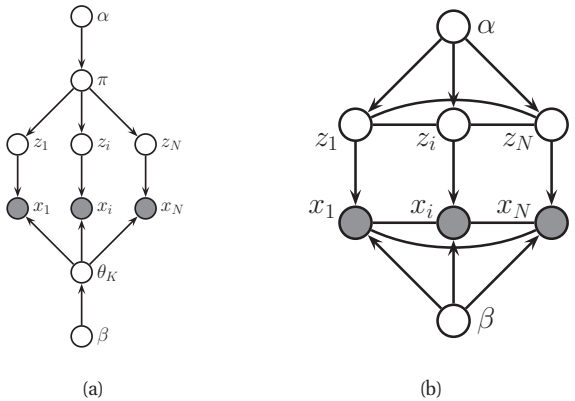

Figure 24.2 (a) A mixture model. (b) After integrating out the parameters.

We will encounter Rao-Blackwellisation again in Section 23.6. Although it can reduce statistical variance, it is only worth doing if the integrating out can be done quickly, otherwise we will not be able to produce as many samples per second as the naive method. We give an example of this below.

24.2.4.1 Example: collapsed Gibbs for fitting a GMM

Consider a GMM with a fully conjugate prior. In this case we can analytically integrate out the model parameters $\boldsymbol{\mu}_k$, $\boldsymbol{\Sigma}_k$ and $\boldsymbol{\pi}$, and just sample the indicators $\mathbf{z}$. Once we integrate out $\boldsymbol{\pi}$, all the z_i nodes become inter-dependent. Similarly, once we integrate out $\boldsymbol{\theta}_k$, all the $\mathbf{x}_i$ nodes become inter-dependent, as shown in Figure 24.2(b). Nevertheless, we can easily compute the full conditionals as follows:

$$
\begin{aligned}
p(z_i = k|\mathbf{z}_{-i}, \mathbf{x}, \boldsymbol{\alpha}, \boldsymbol{\beta}) &\propto p(z_i = k|\mathbf{z}_{-i}, \boldsymbol{\alpha}, \cancel{\boldsymbol{\beta}}) p(\mathbf{x}|z_i = k, \mathbf{z}_{-i}, \cancel{\boldsymbol{\alpha}}, \boldsymbol{\beta}) && (24.21)\\
&\propto p(z_i = k|\mathbf{z}_{-i}, \boldsymbol{\alpha}) p(\mathbf{x}_i|\mathbf{x}_{-i}, z_i = k, \mathbf{z}_{-i}, \boldsymbol{\beta}) \\
&\quad p(\mathbf{x}_{-i}|\cancel{z_i = k}, \mathbf{z}_{-i}, \boldsymbol{\beta}) && (24.22)\\
&\propto p(z_i = k|\mathbf{z}_{-i}, \boldsymbol{\alpha}) p(\mathbf{x}_i|\mathbf{x}_{-i}, z_i = k, \mathbf{z}_{-i}, \boldsymbol{\beta}) && (24.23)
\end{aligned}
$$

where $\boldsymbol{\beta} = (\mathbf{m}_0, \mathbf{V}_0, \mathbf{S}_0, \nu_0)$ are the hyper-parameters for the class-conditional densities. The first term can be obtained by integrating out $\boldsymbol{\pi}$. Suppose we use a symmetric prior of the form $\boldsymbol{\pi} \sim \mathrm{Dir}(\boldsymbol{\alpha})$, where $\alpha_k = \alpha/K$. From Equation 5.26 we have

$$
p(z_1, \ldots, z_N|\alpha) = \frac{\Gamma(\alpha)}{\Gamma(N+\alpha)} \prod_{k=1}^{K} \frac{\Gamma(N_k + \alpha/K)}{\Gamma(\alpha/K)} \tag{24.24}
$$

Hence

$$p(z_i = k|\mathbf{z}_{-i}, \alpha) = \frac{p(\mathbf{z}_{1:N}|\alpha)}{p(\mathbf{z}_{-i}|\alpha)} = \frac{\frac{1}{\Gamma(N+\alpha)}}{\frac{1}{\Gamma(N+\alpha-1)}} \times \frac{\Gamma(N_k + \alpha/K)}{\Gamma(N_{k,-i} + \alpha/K)} \tag{24.25}$$

$$= \frac{\Gamma(N+\alpha-1)}{\Gamma(N+\alpha)} \frac{\Gamma(N_{k,-i} + 1 + \alpha/K)}{\Gamma(N_{k,-i} + \alpha/K)} = \frac{N_{k,-i} + \alpha/K}{N + \alpha - 1} \tag{24.26}$$

where $N_{k,-i} \triangleq \sum_{n \neq i} \mathbb{I}(z_n = k) = N_k - 1$, and where we exploited the fact that $\Gamma(x+1) = x\Gamma(x)$.

To obtain the second term in Equation 24.23, which is the posterior predictive distribution for $\mathbf{x}_i$ given all the other data and all the assignments, we use the fact that

$$p(\mathbf{x}_i|\mathbf{x}_{-i}, \mathbf{z}_{-i}, z_i = k, \boldsymbol{\beta}) = p(\mathbf{x}_i|\mathcal{D}_{-i,k}) \tag{24.27}$$

where $\mathcal{D}_{-i,k} = \{\mathbf{x}_j : z_j = k, j \neq i\}$ is all the data assigned to cluster k except for $\mathbf{x}_i$. If we use a conjugate prior for $\boldsymbol{\theta}_k$, we can compute $p(\mathbf{x}_i|\mathcal{D}_{-i,k})$ in closed form. Furthermore, we can efficiently update these predictive likelihoods by caching the sufficient statistics for each cluster. To compute the above expression, we remove $\mathbf{x}_i$'s statistics from its current cluster (namely z_i), and then evaluate $\mathbf{x}_i$ under each cluster's posterior predictive. Once we have picked a new cluster, we add $\mathbf{x}_i$'s statistics to this new cluster.

Some pseudo-code for one step of the algorithm is shown in Algorithm 1, based on (Sudderth 2006, p94). (We update the nodes in random order to improve the mixing time, as suggested in (Roberts and Sahu 1997).) We can initialize the sample by sequentially sampling from $p(z_i|\mathbf{z}_{1:i-1}, \mathbf{x}_{1:i})$. (See `fmGibbs` for some Matlab code, by Yee-Whye Teh.) In the case of GMMs, both the naive sampler and collapsed sampler take $O(NKD)$ time per step.

Algorithm 24.1: Collapsed Gibbs sampler for a mixture model

```
for each i = 1 : N in random order do
    Remove x_i's sufficient statistics from old cluster z_i ;
    for each k = 1 : K do
        Compute p_k(x_i) ≜ p(x_i|{x_j : z_j = k, j ≠ i}) ;
    Compute p(z_i = k|z_{-i}, D) ∝ (N_{k,-i} + α/K) p_k(x_i);
    Sample z_i ~ p(z_i|·) ;
    Add x_i's sufficient statistics to new cluster z_i
```

A comparison of this method with the standard Gibbs sampler is shown in Figure 24.3. The vertical axis is the data log probability at each iteration, computed using

$$\log p(\mathcal{D}|\mathbf{z}, \boldsymbol{\theta}) = \sum_{i=1}^{N} \log \left[\pi_{z_i} p(\mathbf{x}_i|\boldsymbol{\theta}_{z_i})\right] \tag{24.28}$$

To compute this quantity using the collapsed sampler, we have to sample $\boldsymbol{\theta} = (\boldsymbol{\pi}, \boldsymbol{\theta}_{1:K})$ given the data and the current assignment $\mathbf{z}$.

In Figure 24.3 we see that the collapsed sampler does indeed generally work better than the vanilla sampler. Occasionally, however, both methods can get stuck in poor local modes. (Note

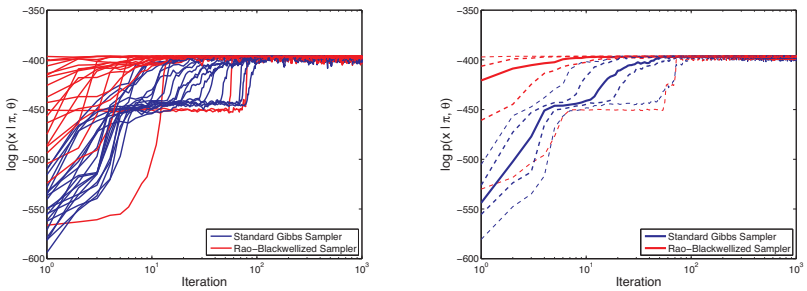

Figure 24.3 Comparison of collapsed (red) and vanilla (blue) Gibbs sampling for a mixture of $K = 4$ two-dimensional Gaussians applied to $N = 300$ data points (shown in Figure 25.7). We plot log probability of the data vs iteration. (a) 20 different random initializations. (b) logprob averaged over 100 different random initializations. Solid line is the median, thick dashed in the 0.25 and 0.75 quantiles, and thin dashed are the 0.05 and 0.95 quintiles. Source: Figure 2.20 of (Sudderth 2006). Used with kind permission of Erik Sudderth.

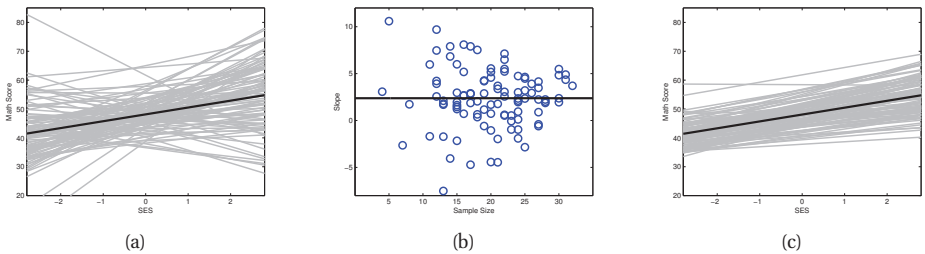

Figure 24.4 (a) Least squares regression lines for math scores vs socio-economic status for 100 schools. Population mean (pooled estimate) is in bold. (b) Plot of $\hat{w}_{2j}$ (the slope) vs N_j (sample size) for the 100 schools. The extreme slopes tend to correspond to schools with smaller sample sizes. (c) Predictions from the hierarchical model. Population mean is in bold. Based on Figure 11.1 of (Hoff 2009). Figure generated by `multilevelLinregDemo`, written by Emtiyaz Khan.

that the error bars in Figure 24.3(b) are averaged over starting values, whereas the theorem refers to MC samples in a single run.)

24.2.5 Gibbs sampling for hierarchical GLMs

Often we have data from multiple related sources. If some sources are more reliable and/or data-rich than others, it makes sense to model all the data simultaneously, so as to enable the borrowing of statistical strength. One of the most natural way to solve such problems is to use hierarchical Bayesian modeling, also called multi-level modeling. In Section 9.6, we discussed a way to perform approximate inference in such models using variational methods. Here we discuss how to use Gibbs sampling.

To explain the method, consider the following example. Suppose we have data on students

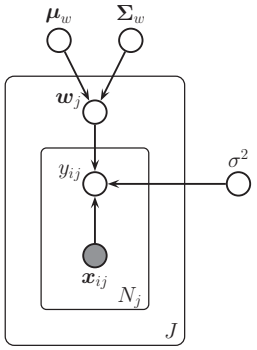

Figure 24.5 Multi-level model for linear regression.

in different schools. Such data is naturally modeled in a two-level hierarchy: we let y_{ij} be the response variable we want to predict for student i in school j. This prediction can be based on school and student specific covariates, $\mathbf{x}_{ij}$. Since the quality of schools varies, we want to use a separate parameter for each school. So our model becomes

$$y_{ij} = \mathbf{x}_{ij}^T \mathbf{w}_j + \epsilon_{ij} \tag{24.29}$$

We will illustrate this model below, using a dataset from (Hoff 2009, p197), where x_{ij} is the socio-economic status (SES) of student i in school y, and y_{ij} is their math score.

We could fit each $\mathbf{w}_j$ separately, but this can give poor results if the sample size of a given school is small. This is illustrated in Figure 24.4(a), which plots the least squares regression line estimated separately for each of the $J = 100$ schools. We see that most of the slopes are positive, but there are a few "errant" cases where the slope is negative. It turns out that the lines with extreme slopes tend to be in schools with small sample size, as shown in Figure 24.4(b). Thus we may not necessarily trust these fits.

We can get better results if we construct a hierarchical Bayesian model, in which the $\mathbf{w}_j$ are assumed to come from a common prior: $\mathbf{w}_j \sim \mathcal{N}(\boldsymbol{\mu}_w, \boldsymbol{\Sigma}_w)$. This is illustrated in Figure 24.5. In this model, the schools with small sample size borrow statistical strength from the schools with larger sample size, because the $\mathbf{w}_j$'s are correlated via the latent common parents $(\boldsymbol{\mu}_w, \boldsymbol{\Sigma}_w)$. (It is crucial that these hyper-parameters be inferrred from data; if they were fixed constants, the $\mathbf{w}_j$ would be conditionally independent, and there would be no information sharing between them.)

To complete the model specification, we must specify priors for the shared parameters. Following (Hoff 2009, p198), we will use the following semi-conjugate forms, for convenience:

$$\boldsymbol{\mu}_w \sim \mathcal{N}(\boldsymbol{\mu}_0, \mathbf{V}_0) \tag{24.30}$$

$$\boldsymbol{\Sigma}_w \sim \mathrm{IW}(\eta_0, \mathbf{S}_0^{-1}) \tag{24.31}$$

$$\sigma^2 \sim \mathrm{IG}(\nu_0/2, \nu_0\sigma_0^2/2) \tag{24.32}$$

Given this, it is simple to show that the full conditionals needed for Gibbs sampling have the

following forms. For the group-specific weights:

$$p(\mathbf{w}_j|\mathcal{D}_j,\boldsymbol{\theta}) = \mathcal{N}(\mathbf{w}_j|\boldsymbol{\mu}_j,\boldsymbol{\Sigma}_j) \tag{24.33}$$
$$\boldsymbol{\Sigma}_j^{-1} = \boldsymbol{\Sigma}^{-1} + \mathbf{X}_j^T\mathbf{X}_j/\sigma^2 \tag{24.34}$$
$$\boldsymbol{\mu}_j = \boldsymbol{\Sigma}_j(\boldsymbol{\Sigma}^{-1}\boldsymbol{\mu} + \mathbf{X}_j^T\mathbf{y}_j/\sigma^2) \tag{24.35}$$

For the overall mean:

$$p(\boldsymbol{\mu}_w|\mathbf{w}_{1:J},\boldsymbol{\Sigma}_w) = \mathcal{N}(\boldsymbol{\mu}|\boldsymbol{\mu}_N,\boldsymbol{\Sigma}_N) \tag{24.36}$$
$$\boldsymbol{\Sigma}_N^{-1} = \mathbf{V}_0^{-1} + J\boldsymbol{\Sigma}^{-1} \tag{24.37}$$
$$\boldsymbol{\mu}_N = \boldsymbol{\Sigma}_N(\mathbf{V}_0^{-1}\boldsymbol{\mu}_0 + J\boldsymbol{\Sigma}^{-1}\overline{\mathbf{w}}) \tag{24.38}$$

where $\overline{\mathbf{w}} = \frac{1}{J}\sum_j \mathbf{w}_j$. For the overall covariance:

$$p(\boldsymbol{\Sigma}_w|\boldsymbol{\mu}_w,\mathbf{w}_{1:J}) = \mathrm{IW}((\mathbf{S}_0+\mathbf{S}_\mu)^{-1},\eta_0+J) \tag{24.39}$$
$$\mathbf{S}_\mu = \sum_j(\mathbf{w}_j-\boldsymbol{\mu}_w)(\mathbf{w}_j-\boldsymbol{\mu}_w)^T \tag{24.40}$$

For the noise variance:

$$p(\sigma^2|\mathcal{D},\mathbf{w}_{1:J}) = \mathrm{IG}([\nu_0+N]/2,[\nu_0\sigma_0^2+\mathrm{SSR}(\mathbf{w}_{1:J})]/2) \tag{24.41}$$
$$\mathrm{SSR}(\mathbf{w}_{1:J}) = \sum_{j=1}^{J}\sum_{i=1}^{N_j}(y_{ij}-\mathbf{w}_j^T\mathbf{x}_{ij})^2 \tag{24.42}$$

Applying Gibbs sampling to our hierarchical model, we get the results shown in Figure 24.4(c). The light gray lines plot the mean of the posterior predictive distribution for each school:

$$\mathbb{E}\left[y_j|\mathbf{x}_{ij}\right] = \mathbf{x}_{ij}^T\hat{\mathbf{w}}_j \tag{24.43}$$

where

$$\hat{\mathbf{w}}_j = \mathbb{E}\left[\mathbf{w}_j|\mathcal{D}\right] \approx \frac{1}{S}\sum_{s=1}^{S}\mathbf{w}_j^{(s)} \tag{24.44}$$

The dark gray line in the middle plots the prediction using the overall mean parameters, $\mathbf{x}_{ij}^T\hat{\boldsymbol{\mu}}_w$. We see that the method has regularized the fits quite nicely, without enforcing too much uniformity. (The amount of shrinkage is controlled by $\boldsymbol{\Sigma}_w$, which in turns depends on the hyper-parameters; in this example, we used vague values.)

24.2.6 BUGS and JAGS

One reason Gibbs sampling is so popular is that it is possible to design general purpose software that will work for almost any model. This software just needs a model specification, usually in the form a directed graphical model (specified in a file, or created with a graphical user interface), and a library of methods for sampling from different kinds of full conditionals. (This can often be done using adaptive rejection sampling, described in Section 23.3.4.) An example

of such a package is **BUGS** (Lunn et al. 2000), which stands for "Bayesian updating using Gibbs Sampling". BUGS is very widely used in biostatistics and social science. Another more recent, but very similar, package is **JAGS** (Plummer 2003), which stands for "Just Another Gibbs Sampler". This uses a similar model specification language to BUGS.

For example, we can describe the model in Figure 24.5 as follows:

```
model {
 for (i in 1:N) {
    for (j in 1:J) {
       y[i,j] ~ dnorm(y.hat[i,j], tau.y)
       y.hat[i,j] <- inprod(W[j, ], X[i, j, ])
    }
}
tau.y <- pow(sigma.y, -2)
sigma.y ~ dunif(0,100)

for (j in 1:J) {
  W[j,] ~ dmnorm(mu, SigmaInv)
}
SigmaInv  ~ dwish(S0[,], eta0)
mu ~ dmnorm(mu0, V0inv)
}
```

We can then just pass this model to BUGS or JAGS, which will generate samples for us. See the webpages for details.

Although this approach is appealing, unfortunately it can be much slower than using hand-written code, especially for complex models. There has been some work on automatically deriving model-specific optimized inference code (Fischer and Schumann 2003), but fast code still typically requires human expertise.

24.2.7 The Imputation Posterior (IP) algorithm

The **Imputation Posterior** or IP algorithm (Tanner and Wong 1987) is a special case of Gibbs sampling in which we group the variables into two classes: hidden variables $\mathbf{z}$ and parameters $\boldsymbol{\theta}$. This should sound familiar: it is basically an MCMC version of EM, where the E step gets replaced by the I step, and the M step gets replaced the P step. This is an example of a more general strategy called **data augmentation**, whereby we introduce auxiliary variables in order to simplify the posterior computations (here the computation of $p(\boldsymbol{\theta}|\mathcal{D})$). See (Tanner 1996; van Dyk and Meng 2001) for more information.

24.2.8 Blocking Gibbs sampling

Gibbs sampling can be quite slow, since it only updates one variable at a time (so-called **single site updating**). If the variables are highly correlated, it will take a long time to move away from the current state. This is illustrated in Figure 24.6, where we illustrate sampling from a 2d Gaussian (see Exercise 24.1 for the details). If the variables are highly correlated, the algorithm

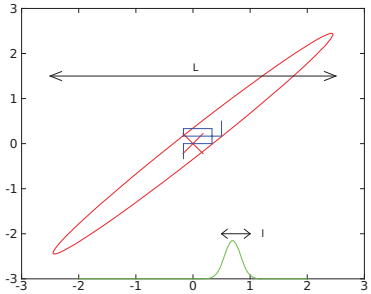

Figure 24.6 Illustration of potentially slow sampling when using Gibbs sampling for a skewed 2D Gaussian. Based on Figure 11.11 of (Bishop 2006b). Figure generated by `gibbsGaussDemo`.

will move very slowly through the state space. In particular, the size of the moves is controlled by the variance of the conditional distributions. If this is ℓ in the x_1 direction, and the support of the distribution is L along this dimension, then we need $O((L/\ell)^2)$ steps to obtain an independent sample.

In some cases we can efficiently sample groups of variables at a time. This is called **blocking Gibbs sampling** or **blocked Gibbs sampling** (Jensen et al. 1995; Wilkinson and Yeung 2002), and can make much bigger moves through the state space.

24.3 Metropolis Hastings algorithm

Although Gibbs sampling is simple, it is somewhat restricted in the set of models to which it can be applied. For example, it is not much help in computing $p(\mathbf{w}|\mathcal{D})$ for a logistic regression model, since the corresponding graphical model has no useful Markov structure. In addition, Gibbs sampling can be quite slow, as we mentioned above.

Fortunately, there is a more general algorithm that can be used, known as the **Metropolis Hastings** or **MH** algorithm, which we describe below.

24.3.1 Basic idea

The basic idea in MH is that at each step, we propose to move from the current state $\mathbf{x}$ to a new state $\mathbf{x}'$ with probability $q(\mathbf{x}'|\mathbf{x})$, where q is called the **proposal distribution** (also called the **kernel**). The user is free to use any kind of proposal they want, subject to some conditions which we explain below. This makes MH quite a flexible method. A commonly used proposal is a symmetric Gaussian distribution centered on the current state, $q(\mathbf{x}'|\mathbf{x}) = \mathcal{N}(\mathbf{x}'|\mathbf{x}, \boldsymbol{\Sigma})$; this is called a **random walk Metropolis algorithm**. We discuss how to choose $\boldsymbol{\Sigma}$ in Section 24.3.3. If we use a proposal of the form $q(\mathbf{x}'|\mathbf{x}) = q(\mathbf{x}')$, where the new state is independent of the old state, we get a method known as the **independence sampler**, which is similar to importance sampling (Section 23.4).

Having proposed a move to $\mathbf{x}'$, we then decide whether to **accept** this proposal or not according to some formula, which ensures that the fraction of time spent in each state is proportional to $p^*(\mathbf{x})$. If the proposal is accepted, the new state is $\mathbf{x}'$, otherwise the new state

is the same as the current state, $\mathbf{x}$ (i.e., we repeat the sample).

If the proposal is symmetric, so $q(\mathbf{x}'|\mathbf{x}) = q(\mathbf{x}|\mathbf{x}')$, the acceptance probability is given by the following formula:

$$r = \min(1, \frac{p^*(\mathbf{x}')}{p^*(\mathbf{x})}) \tag{24.45}$$

We see that if $\mathbf{x}'$ is more probable than $\mathbf{x}$, we definitely move there (since $\frac{p^*(\mathbf{x}')}{p^*(\mathbf{x})} > 1$), but if $\mathbf{x}'$ is less probable, we may still move there anyway, depending on the relative probabilities. So instead of greedily moving to only more probable states, we occasionally allow "downhill" moves to less probable states. In Section 24.3.6, we prove that this procedure ensures that the fraction of time we spend in each state $\mathbf{x}$ is proportional to $p^*(\mathbf{x})$.

If the proposal is asymmetric, so $q(\mathbf{x}'|\mathbf{x}) \neq q(\mathbf{x}|\mathbf{x}')$, we need the **Hastings correction**, given by the following:

$$r = \min(1, \alpha) \tag{24.46}$$

$$\alpha = \frac{p^*(\mathbf{x}')q(\mathbf{x}|\mathbf{x}')}{p^*(\mathbf{x})q(\mathbf{x}'|\mathbf{x})} = \frac{p^*(\mathbf{x}')/q(\mathbf{x}'|\mathbf{x})}{p^*(\mathbf{x})/q(\mathbf{x}|\mathbf{x}')} \tag{24.47}$$

This correction is needed to compensate for the fact that the proposal distribution itself (rather than just the target distribution) might favor certain states.

An important reason why MH is a useful algorithm is that, when evaluating α, we only need to know the target density up to a normalization constant. In particular, suppose $p^*(\mathbf{x}) = \frac{1}{Z}\tilde{p}(\mathbf{x})$, where $\tilde{p}(\mathbf{x})$ is an unnormalized distribution and Z is the normalization constant. Then

$$\alpha = \frac{(\tilde{p}(\mathbf{x}')/Z)\ q(\mathbf{x}|\mathbf{x}')}{(\tilde{p}(\mathbf{x})/Z)\ q(\mathbf{x}'|\mathbf{x})} \tag{24.48}$$

so the Z's cancel. Hence we can sample from p^* even if Z is unknown. In particular, all we have to do is evaluate $\tilde{p}$ pointwise, where $\tilde{p}(\mathbf{x}) = p^*(\mathbf{x})Z$.

The overall algorithm is summarized in Algorithm 2.

24.3.2 Gibbs sampling is a special case of MH

It turns out that Gibbs sampling, which we discussed in Section 24.2, is a special case of MH. In particular, it is equivalent to using MH with a sequence of proposals of the form

$$q(\mathbf{x}'|\mathbf{x}) = p(x_i'|\mathbf{x}_{-i})\mathbb{I}(\mathbf{x}'_{-i} = \mathbf{x}_{-i}) \tag{24.49}$$

That is, we move to a new state where x_i is sampled from its full conditional, but $\mathbf{x}_{-i}$ is left unchanged.

We now prove that the acceptance rate of each such proposal is 1, so the overall algorithm also has an acceptance rate of 100%. We have

$$\alpha = \frac{p(\mathbf{x}')q(\mathbf{x}|\mathbf{x}')}{p(\mathbf{x})q(\mathbf{x}'|\mathbf{x})} = \frac{p(x_i'|\mathbf{x}'_{-i})p(\mathbf{x}'_{-i})p(x_i|\mathbf{x}'_{-i})}{p(x_i|\mathbf{x}_{-i})p(\mathbf{x}_{-i})p(x_i'|\mathbf{x}_{-i})} \tag{24.50}$$

$$= \frac{p(x_i'|\mathbf{x}_{-i})p(\mathbf{x}_{-i})p(x_i|\mathbf{x}_{-i})}{p(x_i|\mathbf{x}_{-i})p(\mathbf{x}_{-i})p(x_i'|\mathbf{x}_{-i})} = 1 \tag{24.51}$$

Algorithm 24.2: Metropolis Hastings algorithm

Initialize x^0 ;
for $s = 0, 1, 2, \ldots$ **do**
  Define $x = x^s$;
  Sample $x' \sim q(x'|x)$;
  Compute acceptance probability

$$\alpha = \frac{\tilde{p}(x')q(x|x')}{\tilde{p}(x)q(x'|x)}$$

  Compute $r = \min(1, \alpha)$;
  Sample $u \sim U(0, 1)$;
  Set new sample to

$$x^{s+1} = \begin{cases} x' & \text{if } u < r \\ x^s & \text{if } u \geq r \end{cases}$$

where we exploited the fact that $\mathbf{x}'_{-i} = \mathbf{x}_{-i}$, and that $q(\mathbf{x}'|\mathbf{x}) = p(x'_i|\mathbf{x}_{-i})$.

The fact that the acceptance rate is 100% does not necessarily mean that Gibbs will converge rapidly, since it only updates one coordinate at a time (see Section 24.2.8). Fortunately, there are many other kinds of proposals we can use, as we discuss below.

24.3.3 Proposal distributions

For a given target distribution p^*, a proposal distribution q is valid or admissible if it gives a non-zero probability of moving to the states that have non-zero probability in the target. Formally, we can write this as

$$\text{supp}(p^*) \subseteq \cup_x \text{supp}(q(\cdot|x)) \tag{24.52}$$

For example, a Gaussian random walk proposal has non-zero probability density on the entire state space, and hence is a valid proposal for any continuous state space.

Of course, in practice, it is important that the proposal spread its probability mass in just the right way. Figure 24.7 shows an example where we use MH to sample from a mixture of two 1D Gaussians using a random walk proposal, $q(x'|x) = \mathcal{N}(x'|x, v)$. This is a somewhat tricky target distribution, since it consists of two well separated modes. It is very important to set the variance of the proposal v correctly: If the variance is too low, the chain will only explore one of the modes, as shown in Figure 24.7(a), but if the variance is too large, most of the moves will be rejected, and the chain will be very **sticky**, i.e., it will stay in the same state for a long time. This is evident from the long stretches of repeated values in Figure 24.7(b). If we set the proposal's variance just right, we get the trace in Figure 24.7(c), where the samples clearly explore the support of the target distribution. We discuss how to tune the proposal below.

One big advantage of Gibbs sampling is that one does not need to choose the proposal

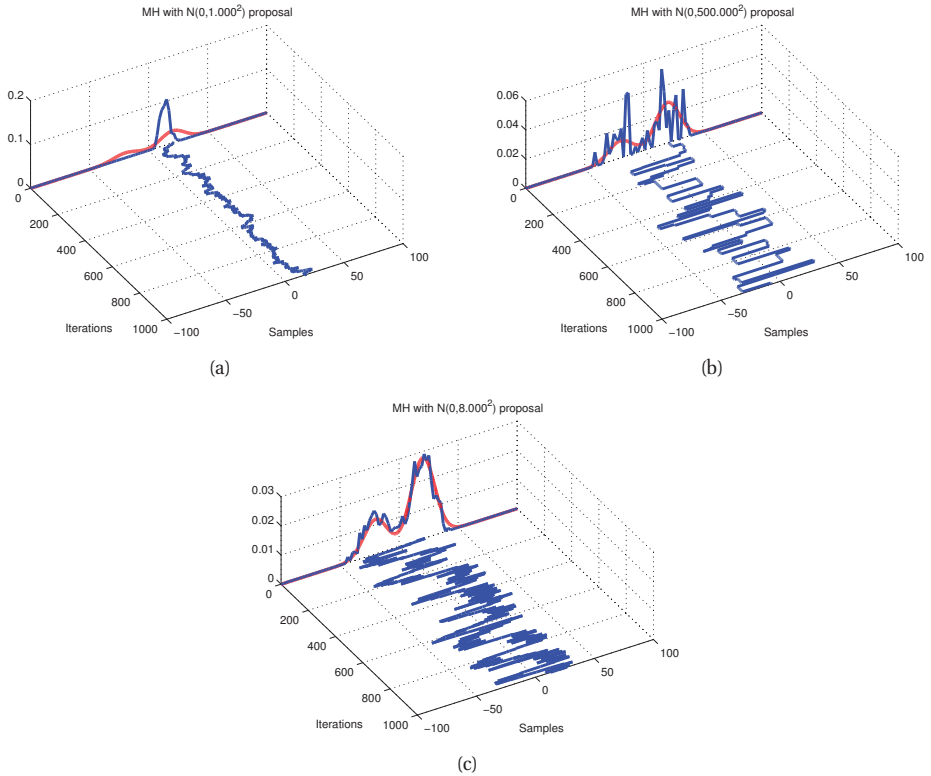

Figure 24.7 An example of the Metropolis Hastings algorithm for sampling from a mixture of two 1D Gaussians ($\boldsymbol{\mu} = (-20, 20)$, $\boldsymbol{\pi} = (0.3, 0.7)$, $\boldsymbol{\sigma} = (100, 100)$), using a Gaussian proposal with variances of $v \in \{1, 500, 8\}$. (a) When $v = 1$, the chain gets trapped near the starting state and fails to sample from the mode at $\mu = -20$. (b) When $v = 500$, the chain is very "sticky", so its effective sample size is low (as reflected by the rough histogram approximation at the end). (c) Using a variance of $v = 8$ is just right and leads to a good approximation of the true distribution (shown in red). Figure generated by `mcmcGmmDemo`. Based on code by Christophe Andrieu and Nando de Freitas.

distribution, and furthermore, the acceptance rate is 100%. Of course, a 100% acceptance can trivially be achieved by using a proposal with variance 0 (assuming we start at a mode), but this is obviously not exploring the posterior. So having a high acceptance is not the ultimate goal. We can increase the amount of exploration by increasing the variance of the Gaussian kernel. Often one experiments with different parameters until the acceptance rate is between 25% and 40%, which theory suggests is optimal, at least for Gaussian target distributions. These short initial runs, used to tune the proposal, are called **pilot runs**.

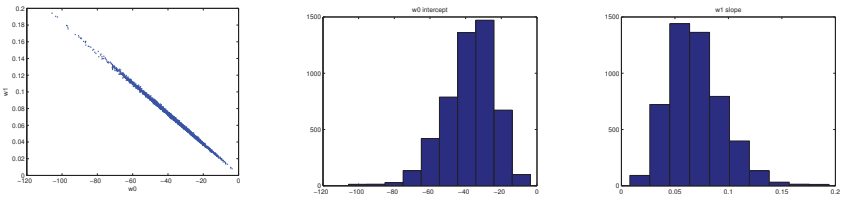

(a) (b) (c)

Figure 24.8 (a) Joint posterior of the parameters for 1d logistic regression when applied to some SAT data. (b) Marginal for the offset w_0. (c) Marginal for the slope w_1. We see that the marginals do not capture the fact that the parameters are highly correlated. Figure generated by `logregSatMhDemo`.

24.3.3.1 Gaussian proposals

If we have a continuous state space, the Hessian $\mathbf{H}$ at a local mode $\hat{\mathbf{w}}$ can be used to define the covariance of a Gaussian proposal distribution. This approach has the advantage that the Hessian models the local curvature and length scales of each dimension; this approach therefore avoids some of the slow mixing behavior of Gibbs sampling shown in Figure 24.6.

There are two obvious approaches: (1) an independence proposal, $q(\mathbf{w}'|\mathbf{w}) = \mathcal{N}(\mathbf{w}'|\hat{\mathbf{w}}, \mathbf{H}^{-1})$ or (2), a random walk proposal, $q(\mathbf{w}'|\mathbf{w}) = \mathcal{N}(\mathbf{w}'|\mathbf{w}, s^2\mathbf{H}^{-1})$, where s^2 is a scale factor chosen to facilitate rapid mixing. (Roberts and Rosenthal 2001) prove that, if the posterior is Gaussian, the asymptotically optimal value is to use $s^2 = 2.38^2/D$, where D is the dimensionality of $\mathbf{w}$; this results in an acceptance rate of 0.234.

For example, consider MH for binary logistic regression. From Equation 8.7, we have that the Hessian of the log-likelihood is $\mathbf{H}_l = \mathbf{X}^T\mathbf{D}\mathbf{X}$, where $\mathbf{D} = \text{diag}(\mu_i(1-\mu_i))$ and $\mu_i = \text{sigm}(\hat{\mathbf{w}}^T\mathbf{x}_i)$. If we assume a Gaussian prior, $p(\mathbf{w}) = \mathcal{N}(\mathbf{0}, \mathbf{V}_0)$, we have $\mathbf{H} = \mathbf{V}_0^{-1} + \mathbf{H}_l$, so the asymptotically optimal Gaussian proposal has the form

$$q(\mathbf{w}'|\mathbf{w}) = \mathcal{N}\left(\mathbf{w}, \frac{2.38^2}{D}\left(\mathbf{V}_0^{-1} + \mathbf{X}^T\mathbf{D}\mathbf{X}\right)^{-1}\right) \tag{24.53}$$

See (Gamerman 1997; Rossi et al. 2006; Fruhwirth-Schnatter and Fruhwirth 2010) for further details. The approach is illustrated in Figure 24.8, where we sample parameters from a 1d logistic regression model fit to some SAT data. We initialize the chain at the mode, computed using IRLS, and then use the above random walk Metropolis sampler.

If you cannot afford to compute the mode or its Hessian $\mathbf{X}\mathbf{D}\mathbf{X}$, an alternative approach, suggested in (Scott 2009), is to approximate the above proposal as follows:

$$q(\mathbf{w}'|\mathbf{w}) = \mathcal{N}\left(\mathbf{w}, \left(\mathbf{V}_0^{-1} + \frac{6}{\pi^2}\mathbf{X}^T\mathbf{X}\right)^{-1}\right) \tag{24.54}$$

24.3.3.2 Mixture proposals

If one doesn't know what kind of proposal to use, one can try a **mixture proposal**, which is a convex combination of base proposals:

$$q(\mathbf{x}'|\mathbf{x}) = \sum_{k=1}^{K} w_k q_k(\mathbf{x}'|\mathbf{x}) \tag{24.55}$$

where w_k are the mixing weights. As long as each q_k is individually valid, the overall proposal will also be valid.

24.3.3.3 Data-driven MCMC

The most efficient proposals depend not just on the previous hidden state, but also the visible data, i.e., they have the form $q(\mathbf{x}'|\mathbf{x}, \mathcal{D})$. This is called **data-driven MCMC** (see e.g., (Tu and Zhu 2002)). To create such proposals, one can sample $(\mathbf{x}, \mathcal{D})$ pairs from the forwards model and then train a discriminative classifier to predict $p(\mathbf{x}|f(\mathcal{D}))$, where $f(\mathcal{D})$ are some features extracted from the visible data.

Typically $\mathbf{x}$ is a high-dimensional vector (e.g., position and orientation of all the limbs of a person in a visual object detector), so it is hard to predict the entire state vector, $p(\mathbf{x}|f(\mathcal{D}))$. Instead we might train a discriminative detector to predict parts of the state-space, $p(x_k|f_k(\mathcal{D}))$, such as the location of just the face of a person. We can then use a proposal of the form

$$q(\mathbf{x}'|\mathbf{x}, \mathcal{D}) = \pi_0 q_0(\mathbf{x}'|\mathbf{x}) + \sum_k \pi_k q_k(x'_k|f_k(\mathcal{D})) \tag{24.56}$$

where q_0 is a standard data-independent proposal (e.g., random walk), and q_k updates the k'th component of the state space. For added efficiency, the discriminative proposals should suggest joint changes to multiple variables, but this is often hard to do.

The overall procedure is a form of **generate and test**: the discriminative proposals $q(\mathbf{x}'|\mathbf{x})$ generate new hypotheses, which are then "tested" by computing the posterior ratio $\frac{p(\mathbf{x}'|\mathcal{D})}{p(\mathbf{x}|\mathcal{D})}$, to see if the new hypothesis is better or worse. By adding an annealing step, one can modify the algorithm to find posterior modes; this is called **simulated annealing**, and is described in Section 24.6.1. One advantage of using the mode-seeking version of the algorithm is that we do not need to ensure the proposal distribution is reversible.

24.3.4 Adaptive MCMC

One can change the parameters of the proposal as the algorithm is running to increase efficiency. This is called **adaptive MCMC**. This allows one to start with a broad covariance (say), allowing large moves through the space until a mode is found, followed by a narrowing of the covariance to ensure careful exploration of the region around the mode.

However, one must be careful not to violate the Markov property; thus the parameters of the proposal should not depend on the entire history of the chain. It turns out that a sufficient condition to ensure this is that the adaption is "faded out" gradually over time. See e.g., (Andrieu and Thoms 2008) for details.

24.3.5 Initialization and mode hopping

It is necessary to start MCMC in an initial state that has non-zero probability. If the model has deterministic constraints, finding such a legal configuration may be a hard problem in itself. It is therefore common to initialize MCMC methods at a local mode, found using an optimizer.

In some domains (especially with discrete state spaces), it is a more effective use of computation time to perform multiple restarts of an optimizer, and to average over these modes, rather than exploring similar points around a local mode. However, in continuous state spaces, the mode contains negligible volume (Section 5.2.1.3), so it is necessary to locally explore around each mode, in order to visit enough posterior probability mass.

24.3.6 Why MH works *

To prove that the MH procedure generates samples from p^*, we have to use a bit of Markov chain theory, so be sure to read Section 17.2.3 first.

The MH algorithm defines a Markov chain with the following transition matrix:

$$p(\mathbf{x}'|\mathbf{x}) = \begin{cases} q(\mathbf{x}'|\mathbf{x})r(\mathbf{x}'|\mathbf{x}) & \text{if } \mathbf{x}' \neq \mathbf{x} \\ q(\mathbf{x}|\mathbf{x}) + \sum_{\mathbf{x}' \neq \mathbf{x}} q(\mathbf{x}'|\mathbf{x})(1 - r(\mathbf{x}'|\mathbf{x})) & \text{otherwise} \end{cases} \tag{24.57}$$

This follows from a case analysis: if you move to $\mathbf{x}'$ from $\mathbf{x}$, you must have proposed it (with probability $q(\mathbf{x}'|\mathbf{x})$) and it must have been accepted (with probability $r(\mathbf{x}'|\mathbf{x})$); otherwise you stay in state $\mathbf{x}$, either because that is what you proposed (with probability $q(\mathbf{x}|\mathbf{x})$), or because you proposed something else (with probability $q(\mathbf{x}'|\mathbf{x})$) but it was rejected (with probability $1 - r(\mathbf{x}'|\mathbf{x})$).

Let us analyse this Markov chain. Recall from Section 17.2.3.4 that a chain satisfies **detailed balance** if

$$p(\mathbf{x}'|\mathbf{x})p^*(\mathbf{x}) = p(\mathbf{x}|\mathbf{x}')p^*(\mathbf{x}') \tag{24.58}$$

We also showed that if a chain satisfies detailed balance, then p^* is its stationary distribution. Our goal is to show that the MH algorithm defines a transition function that satisfies detailed balance and hence that p^* is its stationary distribution. (If Equation 24.58 holds, we say that p^* is an **invariant** distribution wrt the Markov transition kernel q.)

Theorem 24.3.1. *If the transition matrix defined by the MH algorithm (given by Equation 24.57) is ergodic and irreducible, then p^* is its unique limiting distribution.*

Proof. Consider two states $\mathbf{x}$ and $\mathbf{x}'$. Either

$$p^*(\mathbf{x})q(\mathbf{x}'|\mathbf{x}) < p^*(\mathbf{x}')q(\mathbf{x}|\mathbf{x}') \tag{24.59}$$

or

$$p^*(\mathbf{x})q(\mathbf{x}'|\mathbf{x}) > p^*(\mathbf{x}')q(\mathbf{x}|\mathbf{x}') \tag{24.60}$$

We will ignore ties (which occur with probability zero for continuous distributions). Without loss of generality, assume that $p^*(\mathbf{x})q(\mathbf{x}'|\mathbf{x}) > p^*(\mathbf{x}')q(\mathbf{x}|\mathbf{x}')$. Hence

$$\alpha(\mathbf{x}'|\mathbf{x}) = \frac{p^*(\mathbf{x}')q(\mathbf{x}|\mathbf{x}')}{p^*(\mathbf{x})q(\mathbf{x}'|\mathbf{x})} < 1 \tag{24.61}$$

Hence we have $r(\mathbf{x}'|\mathbf{x}) = \alpha(\mathbf{x}'|\mathbf{x})$ and $r(\mathbf{x}|\mathbf{x}') = 1$.

Now to move from $\mathbf{x}$ to $\mathbf{x}'$ we must first propose $\mathbf{x}'$ and then accept it. Hence

$$p(\mathbf{x}'|\mathbf{x}) = q(\mathbf{x}'|\mathbf{x})r(\mathbf{x}'|\mathbf{x}) = q(\mathbf{x}'|\mathbf{x})\frac{p^*(\mathbf{x}')q(\mathbf{x}|\mathbf{x}')}{p^*(\mathbf{x})q(\mathbf{x}'|\mathbf{x})} = \frac{p^*(\mathbf{x}')}{p^*(\mathbf{x})}q(\mathbf{x}|\mathbf{x}') \tag{24.62}$$

Hence

$$p^*(\mathbf{x})p(\mathbf{x}'|\mathbf{x}) = p^*(\mathbf{x}')q(\mathbf{x}|\mathbf{x}') \tag{24.63}$$

The backwards probability is

$$p(\mathbf{x}|\mathbf{x}') = q(\mathbf{x}|\mathbf{x}')r(\mathbf{x}|\mathbf{x}') = q(\mathbf{x}|\mathbf{x}') \tag{24.64}$$

since $r(\mathbf{x}|\mathbf{x}') = 1$. Inserting this into Equation 24.63 we get

$$p^*(\mathbf{x})p(\mathbf{x}'|\mathbf{x}) = p^*(\mathbf{x}')p(\mathbf{x}|\mathbf{x}') \tag{24.65}$$

so detailed balance holds wrt p^*. Hence, from Theorem 17.2.3, p^* is a stationary distribution. Furthermore, from Theorem 17.2.2, this distribution is unique, since the chain is ergodic and irreducible. □

24.3.7 Reversible jump (trans-dimensional) MCMC *

Suppose we have a set of models with different numbers of parameters, e.g., mixture models in which the number of mixture components is unknown. Let the model be denoted by m, and let its unknowns (e.g., parameters) be denoted by $\mathbf{x}_m \in \mathcal{X}_m$ (e.g., $\mathcal{X}_m = \mathbb{R}^{n_m}$, where n_m is the dimensionality of model m). Sampling in spaces of differing dimensionality is called **trans-dimensional MCMC** (Green 2003). We could sample the model indicator $m \in \{1, \ldots, M\}$ and sample all the parameters from the product space $\prod_{m=1}^{M} \mathcal{X}_m$, but this is very inefficient. It is more parsimonious to sample in the union space $\mathcal{X} = \cup_{m=1}^{M}\{m\} \times \mathcal{X}_m$, where we only worry about parameters for the currently active model.

The difficulty with this approach arises when we move between models of different dimensionality. The trouble is that when we compute the MH acceptance ratio, we are comparing densities defined in different dimensionality spaces, which is meaningless. It is like trying to compare a sphere with a circle. The solution, proposed by (Green 1998) and known as **reversible jump MCMC** or **RJMCMC**, is to augment the low dimensional space with extra random variables so that the two spaces have a common measure.

Unfortunately, we do not have space to go into details here. Suffice it to say that the method can be made to work in theory, although it is a bit tricky in practice. If, however, the continuous parameters can be integrated out (resulting in a method called collapsed RJMCMC), much of the difficulty goes away, since we are just left with a discrete state space, where there is no need to worry about change of measure. For example, (Denison et al. 2002) includes many examples of applications of collapsed RJMCMC applied to Bayesian inference fro adaptive basis-function models. They sample basis functions from a fixed set of candidates (e.g., centered on the data points), and integrate out the other parameters analytically. This provides a Bayesian alternative to using RVMs or SVMs.

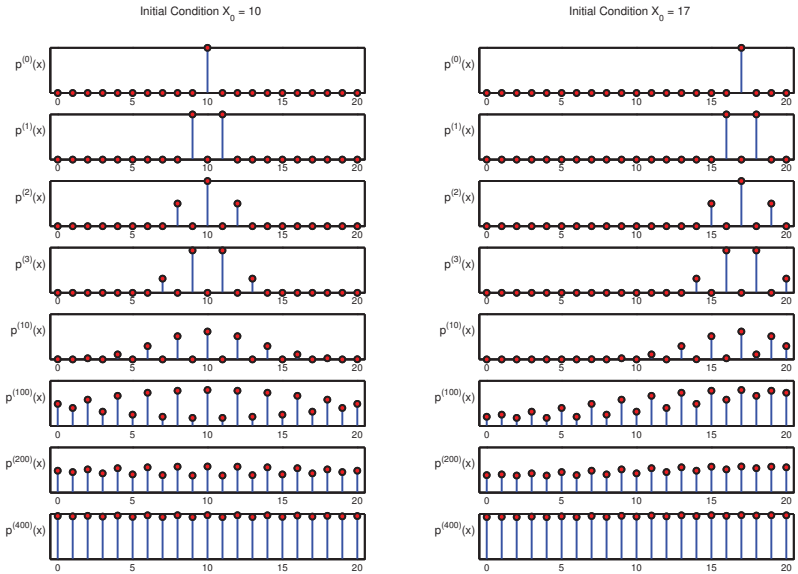

Figure 24.9 Illustration of convergence to the uniform distribution over $\{0, 1, \ldots, 20\}$ using a symmetric random walk starting from (left) state 10, and (right) state 17. Based on Figures 29.14 and 29.15 of (MacKay 2003). Figure generated by `randomWalk0to20Demo`.

24.4 Speed and accuracy of MCMC

In this section, we discuss a number of important theoretical and practical issues to do with MCMC.

24.4.1 The burn-in phase

We start MCMC from an arbitrary initial state. As we explained in Section 17.2.3, only when the chain has "forgotten" where it started from will the samples be coming from the chain's stationary distribution. Samples collected before the chain has reached its stationary distribution do not come from p^*, and are usually thrown away. The initial period, whose samples will be ignored, is called the **burn-in phase**.

For example, consider a uniform distribution on the integers $\{0, 1, \ldots, 20\}$. Suppose we sample from this using a symmetric random walk. In Figure 24.9, we show two runs of the algorithm. On the left, we start in state 10; on the right, we start in state 17. Even in this small problem it takes over 100 steps until the chain has "forgotten" where it started from.

It is difficult to diagnose when the chain has burned in, an issue we discuss in more detail below. (This is one of the fundamental weaknesses of MCMC.) As an interesting example of what can happen if you start collecting samples too early, consider the Potts model. Figure 24.10(a), shows a sample after 500 iterations of Gibbs sampling. This suggests that the model likes

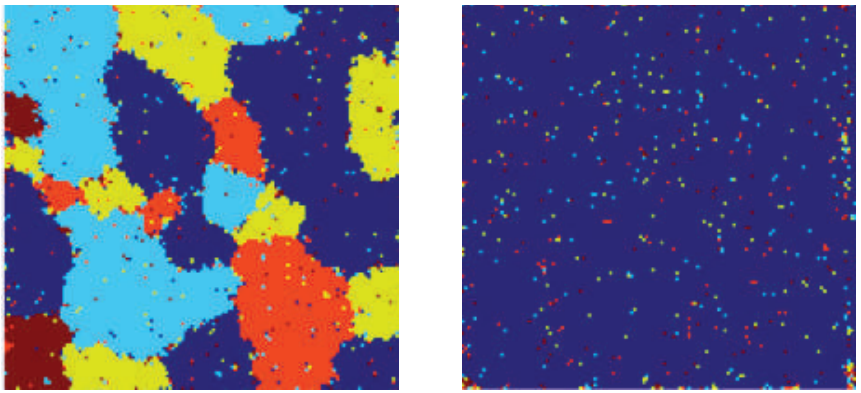

(a) (b)

Figure 24.10 Illustration of problems caused by poor mixing. (a) One sample from a 5-state Potts model on a 128×128 grid with 8 nearest neighbor connectivity and $J = 2/3$ (as in (Geman and Geman 1984)), after 200 iterations. (b) One sample from the same model after 10,000 iterations. Used with kind permission of Erik Sudderth.

medium-sized regions where the label is the same, implying the model would make a good prior for image segmentation. Indeed, this was suggested in the original Gibbs sampling paper (Geman and Geman 1984).

However, it turns out that if you run the chain long enough, you get isolated speckles, as in Figure 24.10(b). The results depend on the coupling strength, but in general, it is very hard to find a setting which produces nice medium-sized blobs: most parameters result in a few super-clusters, or lots of small fragments. In fact, there is a rapid phase transition between these two regimes. This led to a paper called "The Ising/Potts model is not well suited to segmentation tasks" (Morris et al. 1996). It is possible to create priors more suited to image segmentation (e.g., (Sudderth and Jordan 2008)), but the main point here is that sampling before reaching convergence can lead to erroneous conclusions.

24.4.2 Mixing rates of Markov chains *

The amount of time it takes for a Markov chain to converge to the stationary distribution, and forget its initial state, is called the **mixing time**. More formally, we say that the mixing time from state x_0 is the minimal time such that, for any constant $\epsilon > 0$, we have that

$$\tau_\epsilon(x_0) \triangleq \min\{t : ||\delta_{x_0}(x)T^t - p^*||_1 \leq \epsilon\} \tag{24.66}$$

where $\delta_{x_0}(x)$ is a distribution with all its mass in state x_0, T is the transition matrix of the chain (which depends on the target p^* and the proposal q), and $\delta_{x_0}(x)T^t$ is the distribution after t steps. The mixing time of the chain is defined as

$$\tau_\epsilon \triangleq \max_{x_0} \tau_\epsilon(x_0) \tag{24.67}$$

The mixing time is determined by the eigengap $\gamma = \lambda_1 - \lambda_2$, which is the difference of the

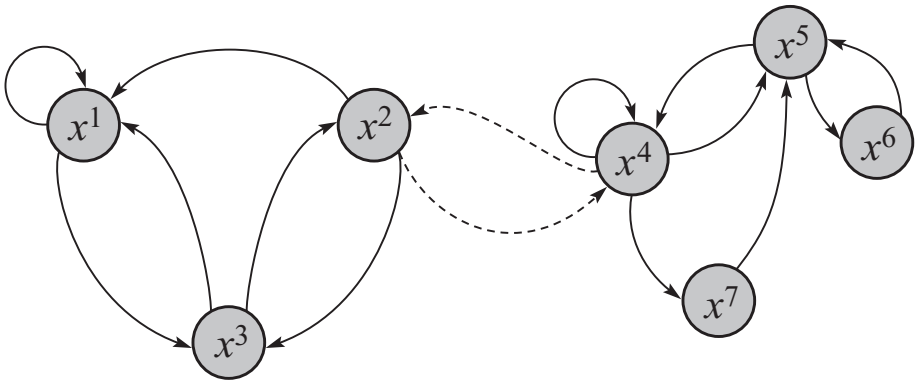

Figure 24.11 A Markov chain with low conductance. The dotted arcs represent transitions with very low probability. Source: Figure 12.6 of (Koller and Friedman 2009). Used with kind permission of Daphne Koller.

first and second eigenvalues of the transition matrix. In particular, one can show that

$$\tau_\epsilon \leq O(\frac{1}{\gamma} \log \frac{n}{\epsilon}) \tag{24.68}$$

where n is the number of states. Since computing the transition matrix can be hard to do, especially for high dimensional and/or continuous state spaces, it is useful to find other ways to estimate the mixing time.

An alternative approach is to examine the geometry of the state space. For example, consider the chain in Figure 24.11. We see that the state space consists of two "islands", each of which is connected via a narrow "bottleneck". (If they were completely disconnected, the chain would not be ergodic, and there would no longer be a unique stationary distribution.) We define the **conductance** ϕ of a chain as the minimum probability, over all subsets of states, of transitioning from that set to its complement:

$$\phi \triangleq \min_{S:0 \leq p^*(S) \leq 0.5} \frac{\sum_{x \in S, x' \in S^c} T(x \to x')}{p^*(S)}, \tag{24.69}$$

One can show that

$$\tau_\epsilon \leq O(\frac{1}{\phi^2} \log \frac{n}{\epsilon}) \tag{24.70}$$

Hence chains with low conductance have high mixing time. For example, distributions with well-separated modes usually have high mixing time. Simple MCMC methods often do not work well in such cases, and more advanced algorithms, such as parallel tempering, are necessary (see e.g., (Liu 2001)).

24.4.3 Practical convergence diagnostics

Computing the mixing time of a chain is in general quite difficult, since the transition matrix is usually very hard to compute. In practice various heuristics have been proposed to diagnose

convergence — see (Geyer 1992; Cowles and Carlin 1996; Brooks and Roberts 1998) for a review. Strictly speaking, these methods do not diagnose convergence, but rather non-convergence. That is, the method may claim the chain has converged when in fact it has not. This is a flaw common to all convergence diagnostics, since diagnosing convergence is computationally intractable in general (Bhatnagar et al. 2010).

One of the simplest approaches to assessing when the method has converged is to run multiple chains from very different **overdispersed** starting points, and to plot the samples of some variables of interest. This is called a **trace plot**. If the chain has mixed, it should have "forgotten" where it started from, so the trace plots should converge to the same distribution, and thus overlap with each other.

Figure 24.12 gives an example. We show the traceplot for x which was sampled from a mixture of two 1D Gaussians using four different methods: MH with a symmetric Gaussian proposal of variance $\sigma^2 \in \{1, 8, 500\}$, and Gibbs sampling. We see that $\sigma^2 = 1$ has not mixed, which is also evident from Figure 24.7(a), which shows that a single chain never leaves the area where it started. The results for the other methods indicate that the chains rapidly converge to the stationary distribution, no matter where they started. (The sticky nature of the $\sigma^2 = 500$ proposal is very evident. This reduces the computational efficiency, as we discuss below, but not the statistical validity.)

24.4.3.1 Estimated potential scale reduction (EPSR)

We can assess convergence more quantitatively as follows. The basic idea is to compare the variance of a quantity within each chain to its variance across chains. More precisely, suppose we collect S samples (after burn-in) from each of C chains of D variables, x_{isc}, $i = 1 : D$, $s = 1 : S$, $c = 1 : C$. Let y_{sc} be a scalar quantity of interest derived from $\mathbf{x}_{1:D,s,c}$ (e.g., $y_{sc} = x_{isc}$ for some chosen i). Define the within-sequence mean and overall mean as

$$\overline{y}_{\cdot c} \triangleq \frac{1}{S}\sum_{s=1}^{S} y_{sc}, \quad \overline{y}_{\cdot\cdot} \triangleq \frac{1}{C}\sum_{c=1}^{C} \overline{y}_{\cdot c} \tag{24.71}$$

Define the between-sequence and within-sequence variance as

$$B \triangleq \frac{S}{C-1}\sum_{c=1}^{C}(\overline{y}_{\cdot c} - \overline{y}_{\cdot\cdot})^2, \quad W \triangleq \frac{1}{C}\sum_{c=1}^{C}\left[\frac{1}{S-1}\sum_{s=1}^{S}(y_{sc} - \overline{y}_{\cdot c})^2\right] \tag{24.72}$$

We can now construct two estimates of the variance of y. The first estimate is W: this should underestimate $\mathrm{var}\,[y]$ if the chains have not ranged over the full posterior. The second estimate is

$$\hat{V} = \frac{S-1}{S}W + \frac{1}{S}B \tag{24.73}$$

This is an estimate of $\mathrm{var}\,[y]$ that is unbiased under stationarity, but is an overestimate if the starting points were overdispersed (Gelman and Rubin 1992). From this, we can define the following convergence diagnostic statistic, known as the **estimated potential scale reduction** or **EPSR**:

$$\hat{R} \triangleq \sqrt{\frac{\hat{V}}{W}} \tag{24.74}$$

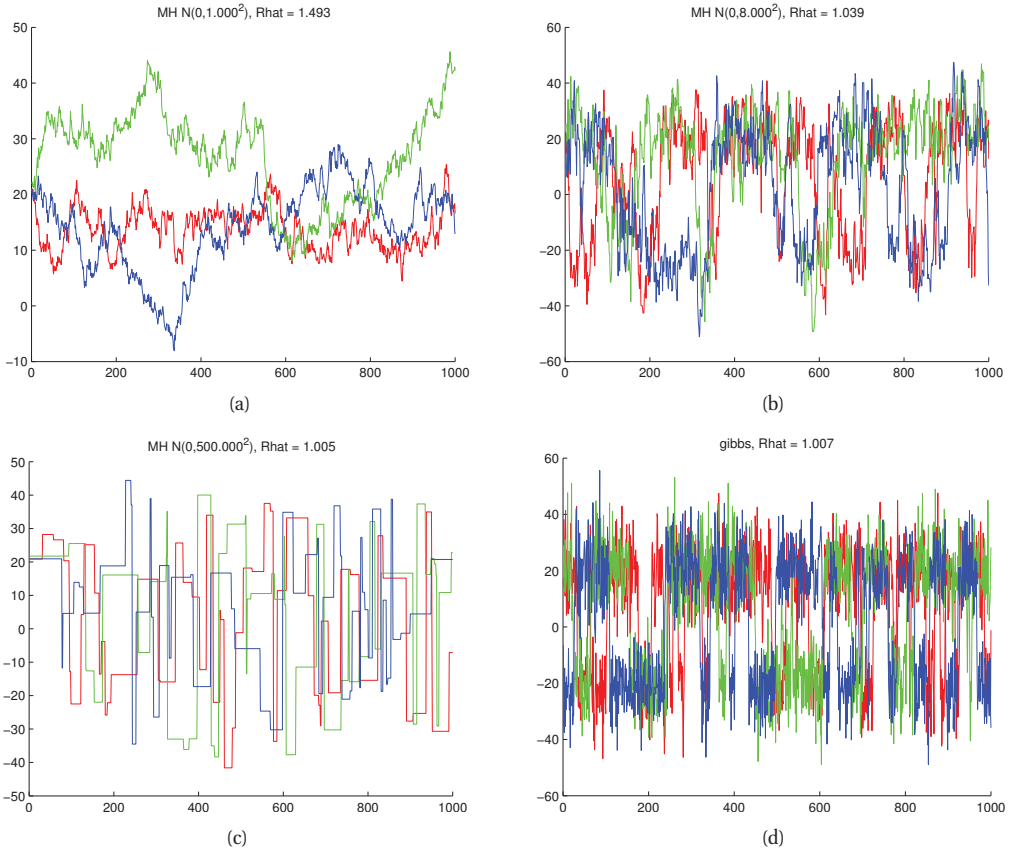

Figure 24.12 Traceplots for MCMC samplers. Each color represents the samples from a different starting point. (a-c) MH with proposal $\mathcal{N}(x'|x, \sigma^2)$ for $\sigma^2 \in \{1, 8, 500\}$, corresponding to Figure 24.7. (d) Gibbs sampling. Figure generated by `mcmcGmmDemo`.

This quantity, which was first proposed in (Gelman and Rubin 1992), measures the degree to which the posterior variance would decrease if we were to continue sampling in the $S \to \infty$ limit. If $\hat{R} \approx 1$ for any given quantity, then that estimate is reliable (or at least is not unreliable). The $\hat{R}$ values for the four samplers in Figure 24.12 are 1.493, 1.039, 1.005 and 1.007. So this diagnostic has correctly identified that the sampler using the first ($\sigma^2 = 1$) proposal is untrustworthy.

24.4.4 Accuracy of MCMC

The samples produced by MCMC are auto-correlated, and this reduces their information content relative to independent or "perfect" samples. We can quantify this as follows.[4] Suppose we want

4. This Section is based on (Hoff 2009, Sec 6.6).

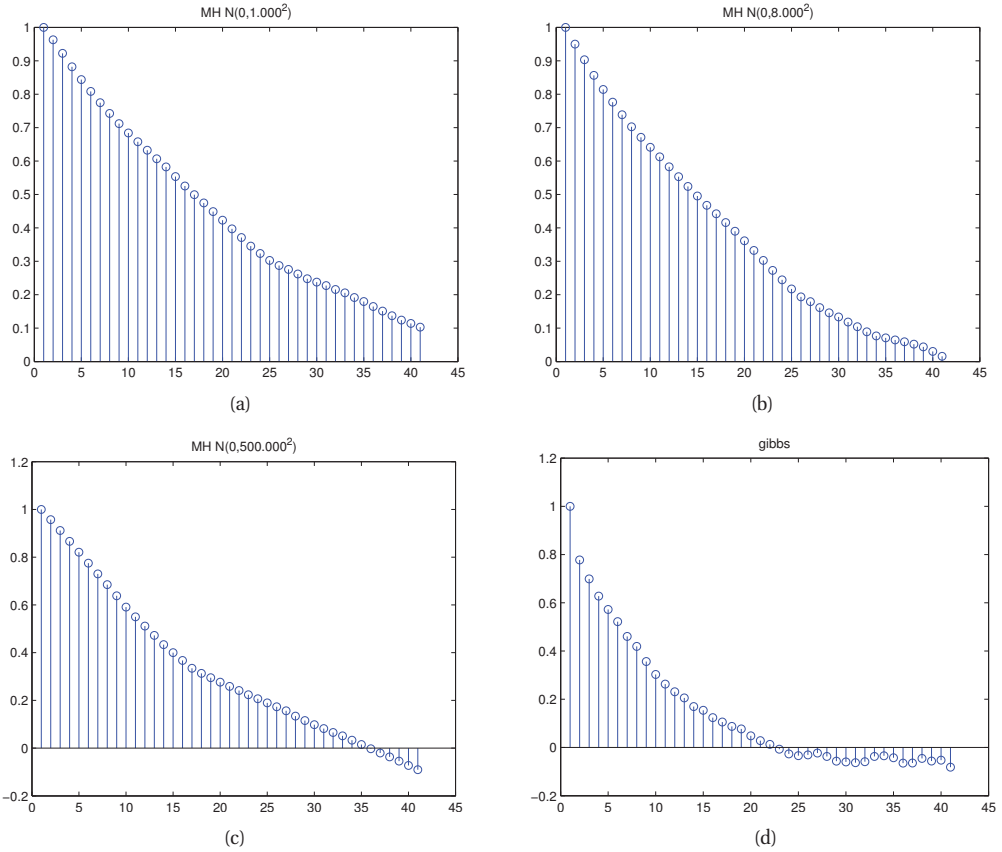

Figure 24.13 Autocorrelation functions corresponding to Figure 24.12. Figure generated by `mcmcGmmDemo`.

to estimate the mean of $f(X)$, for some function f, where $X \sim p()$. Denote the true mean by

$$f^* \triangleq \mathbb{E}\left[f(X)\right] \tag{24.75}$$

A Monte Carlo estimate is given by

$$\overline{f} = \frac{1}{S}\sum_{s=1}^{S} f_s \tag{24.76}$$

where $f_s \triangleq f(x_s)$ and $x_s \sim p(x)$. An MCMC estimate of the variance of this estimate is given by

$$\begin{aligned}
\mathrm{Var}_{MCMC}[\overline{f}] &= \mathbb{E}\left[(\overline{f} - f^*)^2\right] && (24.77)\\
&= \mathbb{E}\left[\left\{\frac{1}{S}\sum_{s=1}^{S}(f_s - f^*)\right\}^2\right] && (24.78)\\
&= \frac{1}{S^2}\mathbb{E}\left[\sum_{s=1}^{S}(f_s - f^*)^2\right] + \frac{1}{S^2}\sum_{s\neq t}\mathbb{E}\left[(f_s - f^*)(f_t - f^*)\right] && (24.79)\\
&= \mathrm{Var}_{MC}(\overline{f}) + \frac{1}{S^2}\sum_{s\neq t}\mathbb{E}\left[(f_s - f^*)(f_t - f^*)\right] && (24.80)
\end{aligned}$$

where the first term is the Monte Carlo estimate of the variance if the samples weren't correlated, and the second term depends on the correlation of the samples. We can measure this as follows. Define the sample-based auto-correlation at lag t of a set of samples $f_1, \ldots, f_S$ as follows:

$$\rho_t \triangleq \frac{\frac{1}{S-t}\sum_{s=1}^{S-t}(f_s - \overline{f})(f_{s+t} - \overline{f})}{\frac{1}{S-1}\sum_{s=1}^{S}(f_s - \overline{f})^2} \tag{24.81}$$

This is called the **autocorrelation function** (ACF). This is plotted in Figure 24.13 for our four samplers for the Gaussian mixture model. We see that the ACF of the Gibbs sampler (bottom right) dies off to 0 much more rapidly than the MH samplers, indicating that each Gibbs sample is "worth" more than each MH sample.

A simple method to reduce the autocorrelation is to use **thinning**, in which we keep every n'th sample. This does not increase the efficiency of the underlying sampler, but it does save space, since it avoids storing highly correlated samples.

We can estimate the information content of a set of samples by computing the **effective sample size** (**ESS**) S_{eff}, defined by

$$S_{\text{eff}} \triangleq \frac{\mathrm{Var}_{MC}(f)}{\mathrm{Var}_{MCMC}(\overline{f})} \tag{24.82}$$

From Figure 24.12, it is clear that the effective sample size of the Gibbs sampler is higher than that of the other samplers (in this example).

24.4.5 How many chains?

A natural question to ask is: how many chains should we run? We could either run one long chain to ensure convergence, and then collect samples spaced far apart, or we could run many short chains, but that wastes the burnin time. In practice it is common to run a medium number of chains (say 3) of medium length (say 100,000 steps), and to take samples from each after discarding the first half of the samples. If we initialize at a local mode, we may be able to use all the samples, and not wait for burn-in.

Model	Goal	Method	Reference
Probit	MAP	Gradient	Section 9.4.1
Probit	MAP	EM	Section 11.4.6
Probit	Post	EP	(Nickisch and Rasmussen 2008)
Probit	Post	Gibbs+	Exercise 24.6
Probit	Post	Gibbs with ARS	(Dellaportas and Smith 1993)
Probit	Post	MH using IRLS proposal	(Gamerman 1997)
Logit	MAP	Gradient	Section 8.3.4
Logit	Post	Gibbs+ with Student	(Fruhwirth-Schnatter and Fruhwirth 2010)
Logit	Post	Gibbs+ with KS	(Holmes and Held 2006)

Table 24.1 Summary of some possible algorithms for estimation and inference for binary classification problems using Gaussian priors. Abbreviations: Aux. = auxiliary variable sampling, ARS = adaptive rejection sampling, EP = expectation propagation, Gibbs+ = Gibbs sampling with auxiliary variables, IRLS = iterative reweighted least squares, KS = Kolmogorov Smirnov, MAP = maximum a posteriori, MH = Metropolis Hastings, Post = posterior.

24.5 Auxiliary variable MCMC *

Sometimes we can dramatically improve the efficiency of sampling by introducing dummy **auxiliary variables**, in order to reduce correlation between the original variables. If the original variables are denoted by $\mathbf{x}$, and the auxiliary variables by $\mathbf{z}$, we require that $\sum_{\mathbf{z}} p(\mathbf{x}, \mathbf{z}) = p(\mathbf{x})$, and that $p(\mathbf{x}, \mathbf{z})$ is easier to sample from than just $p(\mathbf{x})$. If we meet these two conditions, we can sample in the enlarged model, and then throw away the sampled $\mathbf{z}$ values, thereby recovering samples from $p(\mathbf{x})$. We give some examples below.

24.5.1 Auxiliary variable sampling for logistic regression

In Section 9.4.2, we discussed the latent variable interpretation of probit regression. Recall that this had the form

$$z_i \triangleq \mathbf{w}^T \mathbf{x}_i + \epsilon_i \tag{24.83}$$

$$\epsilon_i \sim \mathcal{N}(0, 1) \tag{24.84}$$

$$y_i = 1 = \mathbb{I}(z_i \geq 0) \tag{24.85}$$

We exploited this representation in Section 11.4.6, where we used EM to find an ML estimate. It is straightforward to convert this into an auxiliary variable Gibbs sampler (Exercise 24.6), since $p(\mathbf{w}|\mathcal{D})$ is Gaussian and $p(z_i|\mathbf{x}_i, y_i, \mathbf{w})$ is truncated Gaussian, both of which are easy to sample from.

Now let us discuss how to derive an auxiliary variable Gibbs sampler for logistic regression. Let ϵ_i follow a **logistic distribution**, with pdf

$$p_{\text{Logistic}}(\epsilon) = \frac{e^{-\epsilon}}{(1 + e^{-\epsilon})^2} \tag{24.86}$$

with mean $\mathbb{E}[\epsilon] = 0$ and variance $\text{var}[\epsilon] = \pi^2/3$. The cdf has the form $F(\epsilon) = \text{sigm}(\epsilon)$, which

is the logistic function. Since $y_i = 1$ iff $\mathbf{w}^T\mathbf{x}_i + \epsilon > 0$, we have, by symmetry, that

$$p(y_i = 1|\mathbf{x}_i, \mathbf{w}) = \int_{-\mathbf{w}^T\mathbf{x}_i}^{\infty} f(\epsilon)d\epsilon = \int_{-\infty}^{\mathbf{w}^T\mathbf{x}_i} f(\epsilon)d\epsilon = F(\mathbf{w}^T\mathbf{x}_i) = \text{sigm}(\mathbf{w}^T\mathbf{x}_i) \quad (24.87)$$

as required.

We can derive an auxiliary variable Gibbs sampler by sampling from $p(\mathbf{z}|\mathbf{w}, \mathcal{D})$ and $p(\mathbf{w}|\mathbf{z}, \mathcal{D})$. Unfortunately, sampling directly from $p(\mathbf{w}|\mathbf{z}, \mathcal{D})$ is not possible. One approach is to define $\epsilon_i \sim \mathcal{N}(0, \lambda_i)$, where $\lambda_i = (2\psi_i)^2$ and $\psi_i \sim \text{KS}$, the Kolmogorov Smirnov distribution, and then to sample $\mathbf{w}$, $\mathbf{z}$, $\boldsymbol{\lambda}$ and $\boldsymbol{\psi}$ (Holmes and Held 2006).

A simpler approach is to approximate the logistic distribution by the Student distribution (Albert and Chib 1993). Specifically, we will make the approximation $\epsilon_i \sim \mathcal{T}(0, 1, \nu)$, where $\nu \approx 8$. We can now use the scale mixture of Gaussians representation of the Student to simplify inference. In particular, we write

$$\begin{aligned}
\lambda_i &\sim \text{Ga}(\nu/2, \nu/2) && (24.88)\\
\epsilon_i &\sim \mathcal{N}(0, \lambda_i^{-1}) && (24.89)\\
z_i &\triangleq \mathbf{w}^T\mathbf{x}_i + \epsilon_i && (24.90)\\
y_i = 1|z_i &= \mathbb{I}(z_i \geq 0) && (24.91)
\end{aligned}$$

All of the full conditionals now have a simple form; see Exercise 24.7 for the details.

Note that if we set $\nu = 1$, then $z_i \sim \mathcal{N}(\mathbf{w}^T\mathbf{x}_i, 1)$, which is equivalent to probit regression (see Section 9.4). Rather than choosing between probit or logit regression, we can simply estimate the ν parameter. There is no convenient conjugate prior, but we can consider a finite range of possible values and evaluate the posterior as follows:

$$p(\nu|\boldsymbol{\lambda}) \propto p(\nu) \prod_{i=1}^{N} \frac{1}{\Gamma(\nu/2)(\nu/2)^{\nu/2}} \lambda_i^{\nu/2-1} e^{-\nu\lambda_i/2} \quad (24.92)$$

Furthermore, if we define $\mathbf{V}_0 = v_0\mathbf{I}$, we can sample v_0 as well. For example, suppose we use a $\text{IG}(\delta_1, \delta_2)$ prior for v_0. The posterior is given by $p(v_0|\mathbf{w}) = \text{IG}(\delta_1 + \frac{1}{2}D, \delta_2 + \frac{1}{2}\sum_{j=1}^{D} w_j^2)$. This can be interleaved with the other Gibbs sampling steps, and provides an appealing Bayesian alternative to cross validation for setting the strength of the regularizer.

See Table 24.1 for a summary of various algorithms for fitting probit and logit models. Many of these methods can also be extended to the multinomial logistic regression case. For details, see (Scott 2009; Fruhwirth-Schnatter and Fruhwirth 2010).

24.5.2 Slice sampling

Consider sampling from a univariate, but multimodal, distribution $\tilde{p}(x)$. We can sometimes improve the ability to make large moves by adding an auxiliary variable u. We define the joint distribution as follows:

$$\hat{p}(x, u) = \begin{cases} 1/Z_p & \text{if } 0 \leq u \leq \tilde{p}(x) \\ 0 & \text{otherwise} \end{cases} \quad (24.93)$$

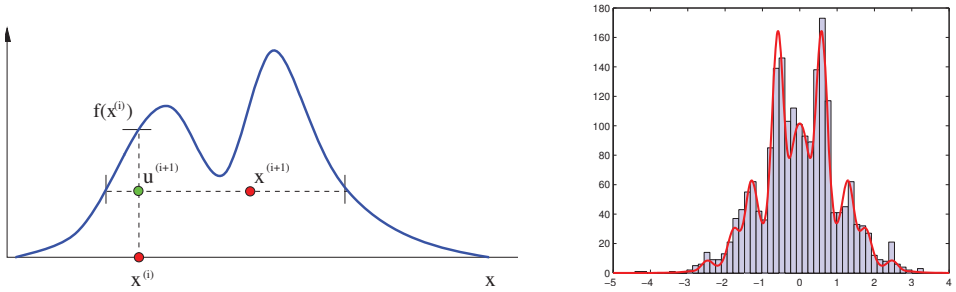

Figure 24.14 (a) Illustration of the principle behind slice sampling. Given a previous sample x^i, we sample u^{i+1} uniformly on $[0, f(x^i)]$, where f is the target density. We then sample x^{i+1} along the slice where $f(x) \geq u^{i+1}$. Source: Figure 15 of (Andrieu et al. 2003) . Used with kind permission of Nando de Freitas. (b) Slice sampling in action. Figure generated by `sliceSamplingDemo1d`.

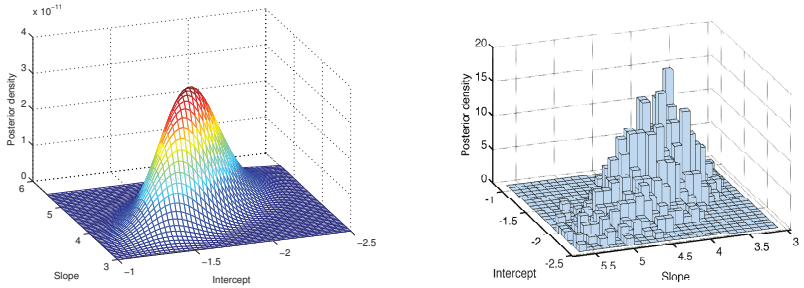

Figure 24.15 Binomial regression for 1d data. (a) Grid approximation to posterior. (b) Slice sampling approximation. Figure generated by `sliceSamplingDemo2d`.

where $Z_p = \int \tilde{p}(x)dx$. The marginal distribution over x is given by

$$\int \hat{p}(x,u)du = \int_0^{\tilde{p}(x)} \frac{1}{Z_p} du = \frac{\tilde{p}(x)}{Z_p} = p(x) \tag{24.94}$$

so we can sample from $p(x)$ by sampling from $\hat{p}(x,u)$ and then ignoring u. The full conditionals have the form

$$p(u|x) = U_{[0,\tilde{p}(x)]}(u) \tag{24.95}$$

$$p(x|u) = U_A(x) \tag{24.96}$$

where $A = \{x : \tilde{p}(x) \geq u\}$ is the set of points on or above the chosen height u. This corresponds to a slice through the distribution, hence the term **slice sampling** (Neal 2003a). See Figure 24.14(a).

In practice, it can be difficult to identify the set A. So we can use the following approach: construct an interval $x_{min} \leq x \leq x_{max}$ around the current point x^s of some width. We then

test to see if each end point lies within the slice. If it does, we keep extending in that direction until it lies outside the slice. This is called **stepping out**. A candidate value x' is then chosen uniformly from this region. If it lies within the slice, it is kept, so $x^{s+1} = x'$. Otherwise we shrink the region such that x' forms one end and such that the region still contains x^s. Then another sample is drawn. We continue in this way until a sample is accepted.

To apply the method to multivariate distributions, we can sample one extra auxiliary variable for each dimension. The advantage of slice sampling over Gibbs is that it does not need a specification of the full-conditionals, just the unnormalized joint. The advantage of slice sampling over MH is that it does not need a user-specified proposal distribution (although it does require a specification of the width of the stepping out interval).

Figure 24.14(b) illustrates the algorithm in action on a synthetic 1d problem. Figure 24.15 illustrates its behavior on a slightly harder problem, namely binomial logistic regression. The model has the form

$$y_i \sim \text{Bin}(n_i, \text{logit}(\beta_1 + \beta_2 x_i)) \tag{24.97}$$

We use a vague Gaussian prior for the β_j's. Figure 24.15(a) shows a grid-based approximation to the posterior, and Figure 24.15(b) shows a sample-based approximation. In this example, the grid is faster to compute, but for any problem with more than 2 dimensions, the grid approach is infeasible.

24.5.3 Swendsen Wang

Consider an Ising model of the following form:

$$p(\mathbf{x}) = \frac{1}{Z} \prod_e f_e(\mathbf{x}_e) \tag{24.98}$$

where $\mathbf{x}_e = (x_i, x_j)$ for edge $e = (i, j)$, $x_i \in \{+1, -1\}$, and the edge factor f_e is defined by $\begin{pmatrix} e^J & e^{-J} \\ e^{-J} & e^J \end{pmatrix}$, where J is the edge strength. Gibbs sampling in such models can be slow when J is large in absolute value, because neighboring states can be highly correlated. The **Swendsen Wang** algorithm (Swendsen and Wang 1987) is a auxiliary variable MCMC sampler which mixes much faster, at least for the case of attractive or ferromagnetic models, with $J > 0$.

Suppose we introduce auxiliary binary variables, one per edge. [5] These are called **bond variables**, and will be denoted by $\mathbf{z}$. We then define an extended model $p(\mathbf{x}, \mathbf{z})$ of the form

$$p(\mathbf{x}, \mathbf{z}) = \frac{1}{Z'} \prod_e g_e(\mathbf{x}_e, z_e) \tag{24.99}$$

where $z_e \in \{0, 1\}$, and we define the new factor as follows: $g_e(\mathbf{x}_e, z_e = 0) = \begin{pmatrix} e^{-J} & e^{-J} \\ e^{-J} & e^{-J} \end{pmatrix}$, and $g_e(\mathbf{x}_e, z_e = 1) = \begin{pmatrix} e^J - e^{-J} & 0 \\ 0 & e^J - e^{-J} \end{pmatrix}$. It is clear that $\sum_{z_e=0}^{1} g_e(\mathbf{x}_e, z_e) = f_e(\mathbf{x}_e)$,

5. Our presentation of the method is based on some notes by David Mackay, available from `http://www.inference.phy.cam.ac.uk/mackay/itila/swendsen.pdf`.

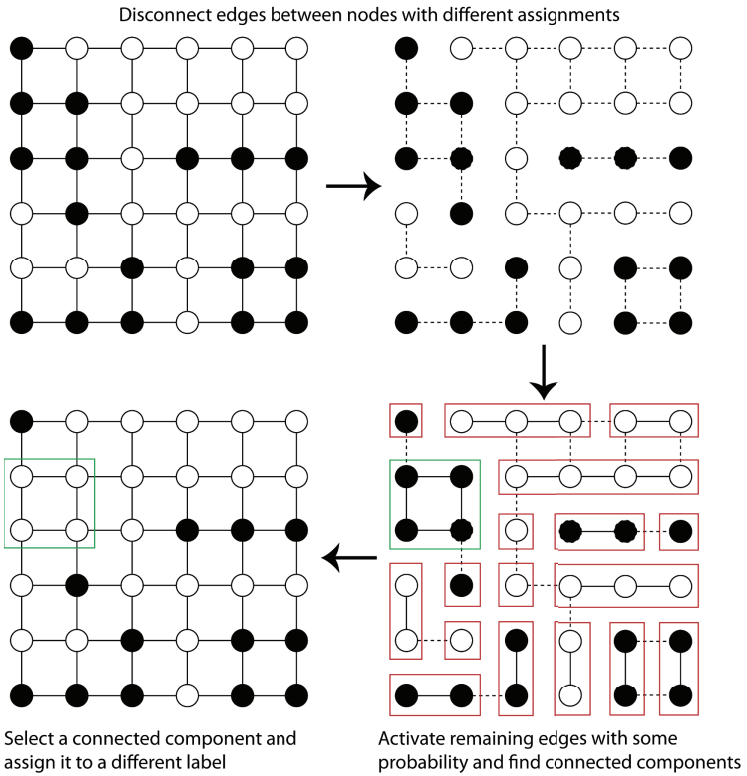

Figure 24.16 Illustration of the Swendsen Wang algorithm on a 2d grid. Used with kind permission of Kevin Tang.

and hence that $\sum_{\mathbf{z}} p(\mathbf{x}, \mathbf{z}) = p(\mathbf{x})$. So if we can sample from this extended model, we can just throw away the $\mathbf{z}$ samples and get valid $\mathbf{x}$ samples from the original distribution.

Fortunately, it is easy to apply Gibbs sampling to this extended model. The full conditional $p(\mathbf{z}|\mathbf{x})$ factorizes over the edges, since the bond variables are conditionally independent given the node variables. Furthermore, the full conditional $p(z_e|\mathbf{x}_e)$ is simple to compute: if the nodes on either end of the edge are in the same state ($x_i = x_j$), we set the bond z_e to 1 with probability $p = 1 - e^{-2J}$, otherwise we set it to 0. In Figure 24.16 (top right), the bonds that could be turned on (because their corresponding nodes are in the same state) are represented by dotted edges. In Figure 24.16 (bottom right), the bonds that are randomly turned on are represented by solid edges.

To sample $p(\mathbf{x}|\mathbf{z})$, we proceed as follows. Find the connected components defined by the graph induced by the bonds that are turned on. (Note that a connected component may consist of a singleton node.) Pick one of these components uniformly at random. All the nodes in each such component must have the same state, since the off-diagonal terms in the $g_e(\mathbf{x}_e, z_e = 1)$ factor are 0. Pick a state ± 1 uniformly at random, and force all the variables in this component to adopt this new state. This is illustrated in Figure 24.16 (bottom left), where the green square

denotes the selected connected component, and we choose to force all nodes within in to enter the white state.

The validity of this algorithm is left as an exercise, as is the extension to handle local evidence and non-stationary potentials.

It should be intuitively clear that Swendsen Wang makes much larger moves through the state space than Gibbs sampling. In fact, SW mixes much faster than Gibbs sampling on 2d lattice Ising models for a variety of values of the coupling parameter, provided $J > 0$. More precisely, let the edge strength be parameterized by J/T, where $T > 0$ is a computational temperature. For large T, the nodes are roughly independent, so both methods work equally well. However, as T approaches a **critical temperature** T_c, the typical states of the system have very long correlation lengths, and Gibbs sampling takes a very long time to generate independent samples. As the temperature continues to drop, the typical states are either all on or all off. The frequency with which Gibbs sampling moves between these two modes is exponentiall small. By contrast, SW mixes rapidly at all temperatures.

Unfortunately, if any of the edge weights are negative, $J < 0$, the system is **frustrated**, and there are exponentially many modes, even at low temperature. SW does not work very well in this setting, since it tries to force many neighboring variables to have the same state. In fact, computation in this regime is provably hard for any algorithm (Jerrum and Sinclair 1993, 1996).

24.5.4 Hybrid/Hamiltonian MCMC *

In this section, we briefly mention a way to perform MCMC sampling for continuous state spaces, for which we can compute the gradient of the (unnormalized) log-posterior. This is the case in neural network models, for example.

The basic idea is to think of the parameters as a particle in space, and to create auxiliary variables which represent the "momentum" of this particle. We then update this parameter/ momentum pair according to certain rules (see e.g., (Duane et al. 1987; Neal 1993; MacKay 2003; Neal 2010) for details). The resulting method is called **hybrid MCMC** or **Hamiltonian MCMC**. The two main parameters that the user must specify are how many **leapfrog steps** to take when updating the position/ momentum, and how big to make these steps. Performance can be quite sensitive to these parameters (although see (Hoffman and Gelman 2011) for a recent way to set them automatically). This method can be combined with stochastic gradient descent (Section 8.5.2) in order to handle large datasets, as explained in (Ahn et al. 2012).

Recently, a more powerful extension of this method has been developed, that exploits second-order gradient information. See (Girolami et al. 2010) for details.

24.6 Annealing methods

Many distributions are multimodal and hence hard to sample from. However, by analogy to the way metals are heated up and then cooled down in order to make the molecules align, we can imagine using a computational temperature parameter to smooth out a distribution, gradually cooling it to recover the original "bumpy" distribution. We first explain this idea in more detail in the context of an algorithm for MAP estimation. We then discuss extensions to the sampling case.

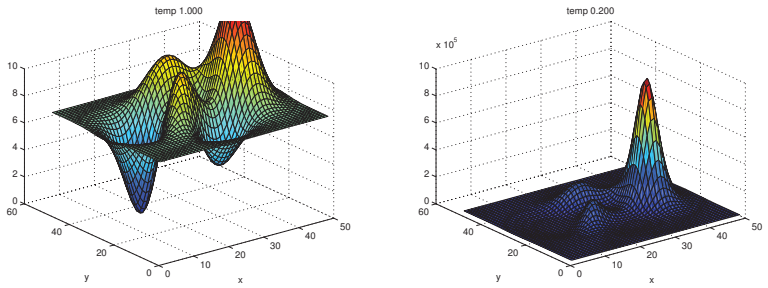

(a) (b)

Figure 24.17 An energy surface at different temperatures. Note the different vertical scales. (a) $T = 1$. (b) $T = 0.5$. Figure generated by `saDemoPeaks`.

24.6.1 Simulated annealing

Simulated annealing (Kirkpatrick et al. 1983) is a stochastic algorithm that attempts to find the global optimum of a black-box function $f(\mathbf{x})$. It is closely related to the Metropolis-Hastings algorithm for generating samples from a probability distribution, which we discussed in Section 24.3. SA can be used for both discrete and continuous optimization.

The method is inspired by statistical physics. The key quantity is the **Boltzmann distribution**, which specifies that the probability of being in any particular state $\mathbf{x}$ is given by

$$p(\mathbf{x}) \propto \exp(-f(\mathbf{x})/T) \tag{24.100}$$

where $f(\mathbf{x})$ is the "energy" of the system and T is the computational temperature. As the temperature approaches 0 (so the system is cooled), the system spends more and more time in its minimum energy (most probable) state.

Figure 24.17 gives an example of a 2d function at different temperatures. At high temperatures, $T \gg 1$, the surface is approximately flat, and hence it is easy to move around (i.e., to avoid local optima). As the temperature cools, the largest peaks become larger, and the smallest peaks disappear. By cooling slowly enough, it is possible to "track" the largest peak, and thus find the global optimum. This is an example of a **continuation method**.

We can generate an algorithm from this as follows. At each step, sample a new state according to some proposal distribution $\mathbf{x}' \sim q(\cdot|\mathbf{x}_k)$. For real-valued parameters, this is often simply a random walk proposal, $\mathbf{x}' = \mathbf{x}_k + \boldsymbol{\epsilon}_k$, where $\boldsymbol{\epsilon}_k \sim \mathcal{N}(\mathbf{0}, \boldsymbol{\Sigma})$. For discrete optimization, other kinds of local moves must be defined.

Having proposed a new state, we compute

$$\alpha = \exp\left((f(\mathbf{x}) - f(\mathbf{x}'))/T\right) \tag{24.101}$$

We then accept the new state (i.e., set $\mathbf{x}_{k+1} = \mathbf{x}'$) with probability $\min(1, \alpha)$, otherwise we stay in the current state (i.e., set $\mathbf{x}_{k+1} = \mathbf{x}_k$). This means that if the new state has lower energy (is more probable), we will definitely accept it, but it it has higher energy (is less probable), we might still accept, depending on the current temperature. Thus the algorithm allows "down-hill" moves in probability space (up-hill in energy space), but less frequently as the temperature drops.

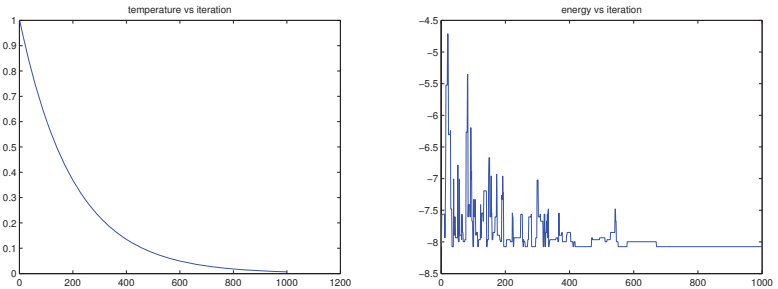

Figure 24.18 A run of simulated annealing on the energy surface in Figure 24.17. (a) Temperature vs iteration. (b) Energy vs iteration. Figure generated by `saDemoPeaks`.

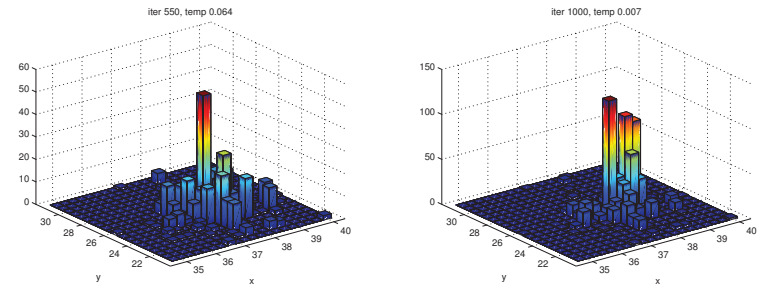

Figure 24.19 Histogram of samples from the annealed "posterior" at 2 different time points produced by simulated annealing on the energy surface shown in Figure 24.17. Note that at cold temperatures, most of the samples are concentrated near the peak at (38,25). Figure generated by `saDemoPeaks`.

The rate at which the temperature changes over time is called the **cooling schedule**. It has been shown (Kirkpatrick et al. 1983) that if one cools sufficiently slowly, the algorithm will provably find the global optimum. However, it is not clear what "sufficient slowly" means. In practice it is common to use an **exponential cooling schedule** of the following form: $T_k = T_0 C^k$, where T_0 is the initial temperature (often $T_0 \sim 1$) and C is the cooling rate (often $C \sim 0.8$). See Figure 24.18(a) for a plot of this cooling schedule. Cooling too quickly means one can get stuck in a local maximum, but cooling too slowly just wastes time. The best cooling schedule is difficult to determine; this is one of the main drawbacks of simulated annealing.

Figure 24.18(b) shows an example of simulated annealing applied to the function in Figure 24.17 using a random walk proposal. We see that the method stochastically reduces the energy over time. Figures 24.19 illustrate (a histogram of) samples drawn from the cooled probability distribution over time. We see that most of the samples are concentrated near the global maximum. When the algorithm has converged, we just return the largest value found.

24.6.2 Annealed importance sampling

We now describe a method known as **annealed importance sampling** (Neal 2001) that combines ideas from simulated annealing and importance sampling in order to draw independent samples from difficult (e.g., multimodal) distributions.

Suppose we want to sample from $p_0(\mathbf{x}) \propto f_0(\mathbf{x})$, but we cannot do so easily; for example, this might represent a multimodal posterior. Suppose however that there is an easier distribution which we can sample from, call it $p_n(\mathbf{x}) \propto f_n(\mathbf{x})$; for example, this might be the prior. We can now construct a sequence of intermediate distributions than move slowly from p_n to p_0 as follows:

$$f_j(\mathbf{x}) = f_0(\mathbf{x})^{\beta_j} f_n(\mathbf{x})^{1-\beta_j} \tag{24.102}$$

where $1 = \beta_0 > \beta_1 > \cdots > \beta_n = 0$, where β_j is an inverse temperature. (Contrast this to the scheme used by simulated annealing which has the form $f_j(\mathbf{x}) = f_0(\mathbf{x})^{\beta_j}$; this makes it hard to sample from p_n.) Furthermore, suppose we have a series of Markov chains $T_j(\mathbf{x}, \mathbf{x}')$ (from $\mathbf{x}$ to $\mathbf{x}'$) which leave each p_j invariant. Given this, we can sample $\mathbf{x}$ from p_0 by first sampling a sequence $\mathbf{z} = (\mathbf{z}_{n-1}, \ldots, \mathbf{z}_0)$ as follows: sample $\mathbf{z}_{n-1} \sim p_n$; sample $\mathbf{z}_{n-2} \sim T_{n-1}(\mathbf{z}_{n-1}, \cdot)$; ...; sample $\mathbf{z}_0 \sim T_1(\mathbf{z}_1, \cdot)$. Finally we set $\mathbf{x} = \mathbf{z}_0$ and give it weight

$$w = \frac{f_{n-1}(\mathbf{z}_{n-1})}{f_n(\mathbf{z}_{n-1})} \frac{f_{n-2}(\mathbf{z}_{n-2})}{f_{n-1}(\mathbf{z}_{n-2})} \cdots \frac{f_1(\mathbf{z}_1)}{f_2(\mathbf{z}_1)} \frac{f_0(\mathbf{z}_0)}{f_1(\mathbf{z}_0)} \tag{24.103}$$

This can be shown to be correct by viewing the algorithm as a form of importance sampling in an extended state space $\mathbf{z} = (\mathbf{z}_0, \ldots, \mathbf{z}_{n-1})$. Consider the following distribution on this state space:

$$p(\mathbf{z}) \propto f(\mathbf{z}) = f_0(\mathbf{z}_0)\tilde{T}_1(\mathbf{z}_0, \mathbf{z}_1)\tilde{T}_2(\mathbf{z}_1, \mathbf{z}_2) \cdots \tilde{T}_{n-1}(\mathbf{z}_{n-2}, \mathbf{z}_{n-1}) \tag{24.104}$$

where $\tilde{T}_j$ is the reversal of T_j:

$$\tilde{T}_j(\mathbf{z}, \mathbf{z}') = T_j(\mathbf{z}', \mathbf{z}) p_j(\mathbf{z}')/p_j(\mathbf{z}) = T_j(\mathbf{z}', \mathbf{z}) f_j(\mathbf{z}')/f_j(\mathbf{z}) \tag{24.105}$$

It is clear that $\sum_{\mathbf{z}_1, \ldots, \mathbf{z}_{n-1}} f(\mathbf{z}) = f_0(\mathbf{z}_0)$, so we can safely just use the $\mathbf{z}_0$ part of these sequences to recover the original ditribution.

Now consider the proposal distribution defined by the algorithm:

$$q(\mathbf{z}) \propto g(\mathbf{z}) = f_n(\mathbf{z}_{n-1}) T_{n-1}(\mathbf{z}_{n-1}, \mathbf{z}_{n-2}) \cdots T_2(\mathbf{z}_2, \mathbf{z}_1) T_1(\mathbf{z}_1, \mathbf{z}_0) \tag{24.106}$$

One can show that the importance weights $w = \frac{f(\mathbf{z}_0, \ldots, \mathbf{z}_{n-1})}{g(\mathbf{z}_0, \ldots, \mathbf{z}_{n-1})}$ are given by Equation 24.103.

24.6.3 Parallel tempering

Another way to combine MCMC and annealing is to run multiple chains in parallel at different temperatures, and allow one chain to sample from another chain at a neighboring temperature. In this way, the high temperature chain can make long distance moves through the state space, and have this influence lower temperature chains. This is known as **parallel tempering**. See e.g., (Earl and Deem 2005) for details.

24.7 Approximating the marginal likelihood

The marginal likelihood $p(\mathcal{D}|M)$ is a key quantity for Bayesian model selection, and is given by

$$p(\mathcal{D}|M) = \int p(\mathcal{D}|\boldsymbol{\theta}, M)p(\boldsymbol{\theta}|M)d\boldsymbol{\theta} \tag{24.107}$$

Unfortunately, this integral is often intractable to compute, for example if we have non conjugate priors, and/or we have hidden variables. In this section, we briefly discuss some ways to approximate this expression using Monte Carlo. See (Gelman and Meng 1998) for a more extensive review.

24.7.1 The candidate method

There is a simple method for approximating the marginal likelihood known as the **Candidate method** (Chib 1995). This exploits the following identity:

$$p(\mathcal{D}|M) = \frac{p(\mathcal{D}|\boldsymbol{\theta}, M)p(\boldsymbol{\theta}|M)}{p(\boldsymbol{\theta}|\mathcal{D}, M)} \tag{24.108}$$

This holds for any value of $\boldsymbol{\theta}$. Once we have picked some value, we can evaluate $p(\mathcal{D}|\boldsymbol{\theta}, M)$ and $p(\boldsymbol{\theta}|M)$ quite easily. If we have some estimate of the posterior near $\boldsymbol{\theta}$, we can then evaluate the denominator as well. This posterior is often approximated using MCMC.

The flaw with this method is that it relies on the assumption that $p(\boldsymbol{\theta}|\mathcal{D}, M)$ has marginalized over all the modes of the posterior, which in practice is rarely possible. Consequently the method can give very inaccurate results in practice (Neal 1998).

24.7.2 Harmonic mean estimate

Newton and Raftery (1994) proposed a simple method for approximating $p(\mathcal{D})$ using the output of MCMC, as follows:

$$1/p(\mathcal{D}) \approx \frac{1}{S}\sum_{s=1}^{S}\frac{1}{p(\mathcal{D}|\boldsymbol{\theta}^s)} \tag{24.109}$$

where $\boldsymbol{\theta}^s \sim p(\boldsymbol{\theta}|\mathcal{D})$. This expression is the harmonic mean of the likelihood of the data under each sample. The theoretical correctness of this expression follows from the following identity:

$$\int \frac{1}{p(\mathcal{D}|\boldsymbol{\theta})}p(\boldsymbol{\theta}|\mathcal{D})d\boldsymbol{\theta} = \int \frac{1}{p(\mathcal{D}|\boldsymbol{\theta})}\frac{p(\mathcal{D}|\boldsymbol{\theta})p(\boldsymbol{\theta})}{p(\mathcal{D})}d\boldsymbol{\theta} = \frac{1}{p(\mathcal{D})}\int p(\boldsymbol{\theta}|\mathcal{D})d\boldsymbol{\theta} = \frac{1}{p(\mathcal{D})} \tag{24.110}$$

Unfortunately, in practice this method works very poorly. Indeed, Radford Neal called this "the worst Monte Carlo method ever".[6]. The reason it is so bad is that it depends only on samples drawn from the posterior. But the posterior is often very insensitive to the prior, whereas the marginal likelihood is not. We only mention this method in order to warn against its use. We present a better method below.

6. Source: radfordneal.wordpress.com/2008/08/17/the-harmonic-mean-of-the-likelihood-worst-monte-carlo-method-ever.

24.7.3 Annealed importance sampling

We can use annealed importance sampling (Section 24.6.2) to evaluate a ratio of partition functions. Notice that $Z_0 = \int f_0(\mathbf{x})d\mathbf{x} = \int f(\mathbf{z})d\mathbf{z}$, and $Z_n = \int f_n(\mathbf{x})d\mathbf{x} = \int g(\mathbf{z})d\mathbf{z}$. Hence

$$\frac{Z_0}{Z_n} = \frac{\int f(\mathbf{z})d\mathbf{z}}{\int g(\mathbf{z})d\mathbf{z}} = \frac{\int \frac{f(\mathbf{z})}{g(\mathbf{z})} g(\mathbf{z})d\mathbf{z}}{\int g(\mathbf{z})d\mathbf{z}} = \mathbb{E}_q\left[\frac{f(\mathbf{z})}{g(\mathbf{z})}\right] \approx \frac{1}{S}\sum_{s=1}^{S} w_s \tag{24.111}$$

If f_n is a prior and f_0 is the posterior, we can estimate $Z_n = p(\mathcal{D})$ using the above equation, provided the prior has a known normalization constant Z_0. This is generally considered the method of choice for evaluating difficult partition functions.

Exercises

Exercise 24.1 Gibbs sampling from a 2D Gaussian

Suppose $\mathbf{x} \sim \mathcal{N}(\boldsymbol{\mu}, \boldsymbol{\Sigma})$, where $\boldsymbol{\mu} = (1, 1)$ and $\boldsymbol{\Sigma} = (1, -0.5; -0.5, 1)$. Derive the full conditionals $p(x_1|x_2)$ and $p(x_2|x_1)$. Implement the algorithm and plot the 1d marginals $p(x_1)$ and $p(x_2)$ as histograms. Superimpose a plot of the exact marginals.

Exercise 24.2 Gibbs sampling for a 1D Gaussian mixture model

Consider applying Gibbs sampling to a univariate mixture of Gaussians, as in Section 24.2.3. Derive the expressions for the full conditionals. Hint: if we know $z_n = j$ (say), then μ_j gets "connected" to x_n, but all other values of μ_i, for all $i \neq j$, are irrelevant. (This is an example of context-specific independence, where the structure of the graph simplifies once we have assigned values to some of the nodes.) Hence, given all the z_n values, the posteriors of the μ's should be independent, so the conditional of μ_j should be independent of $\boldsymbol{\mu}_{-j}$. (Similarly for σ_j.)

Exercise 24.3 Gibbs sampling from the Potts model

Modify the code in `gibbsDemoIsing` to draw samples from a Potts prior at different temperatures, as in Figure 19.8.

Exercise 24.4 Full conditionals for hierarchical model of Gaussian means

Let us reconsider the Gaussian-Gaussian model in Section 5.6.2 for modelling multiple related mean parameters θ_j. In this exercise we derive a Gibbs sampler instead of using EB. Suppose, following (Hoff 2009, p134)), that we use the following conjugate priors on the hyper-parameters:

$$\mu \sim \mathcal{N}(\mu_0, \gamma_0^2) \tag{24.112}$$

$$\tau^2 \sim \mathrm{IG}(\eta_0/2, \eta_0\tau_0^2/2) \tag{24.113}$$

$$\sigma^2 \sim \mathrm{IG}(\nu_0/2, \nu_0\sigma_0^2/2) \tag{24.114}$$

We can set $\boldsymbol{\eta} = (\mu_0, \gamma_0, \eta_0, \tau_0, \nu_0, \sigma_0)$ to uninformative values. Given this model specification, show that the full conditionals for μ, τ, σ and the θ_j are as follows:

$$p(\mu|\theta_{1:D}, \tau^2) = \mathcal{N}(\mu|\frac{D\overline{\theta}/\tau^2 + \mu_0/\gamma_0^2}{D/\tau^2 + 1/\gamma_0^2}, [D/\tau^2 + 1/\gamma_0^2]^{-1}) \quad (24.115)$$

$$p(\theta_j|\mu, \tau^2, \mathcal{D}_j, \sigma^2) = \mathcal{N}(\theta_j|\frac{N_j\overline{x}_j/\sigma^2 + 1/\tau^2}{N_j/\sigma^2 + 1/\tau^2}, [N_j/\sigma^2 + 1/\tau^2]^{-1}) \quad (24.116)$$

$$p(\tau^2|\theta_{1:D}, \mu) = \mathrm{IG}(\tau^2|\frac{\eta_0 + D}{2}, \frac{\eta_0\tau_0^2 + \sum_j(\theta_j - \mu)^2}{2}) \quad (24.117)$$

$$p(\sigma^2|\boldsymbol{\theta}_{1:D}, \mathcal{D}) = \mathrm{IG}(\sigma^2|\frac{1}{2}[\nu_0 + \sum_{j=1}^{D} N_j], \frac{1}{2}[\nu_0\sigma_0^2 + \sum_{j=1}^{D}\sum_{i=1}^{N_j}(x_{ij} - \theta_j)^2]) \quad (24.118)$$

Exercise 24.5 Gibbs sampling for robust linear regression with a Student t likelihood

Modify the EM algorithm in Exercise 11.12 to perform Gibbs sampling for $p(\mathbf{w}, \sigma^2, \mathbf{z}|\mathcal{D}, \nu)$.

Exercise 24.6 Gibbs sampling for probit regression

Modify the EM algorithm in Section 11.4.6 to perform Gibbs sampling for $p(\mathbf{w}, \mathbf{z}|\mathcal{D})$. Hint: we can sample from a truncated Gaussian, $\mathcal{N}(z|\mu, \sigma)\mathbb{I}(a \leq z \leq b)$ in two steps: first sample $u \sim U(\Phi((a - \mu)/\sigma), \Phi((b - \mu)/\sigma))$, then set $z = \mu + \sigma\Phi^{-1}(u)$ (Robert 1995).

Exercise 24.7 Gibbs sampling for logistic regression with the Student approximation

Derive the full conditionals for the joint model defined by Equations 24.88 to 24.91.